Results

Part1: Construction of biobricks

Basic parts:

HU: BBa_K1932000

The B. *longum* hup gene encodes the histone-like HU family protein HB1.

We retrieved the sequence information of Hu promoter from NCBI, and have it synthesized and cloned into a pGH vector by a biotechnology company, Generay Biotechnology. This plasmid was cut with restriction enzymes, EcoRI and PstI (Fig.1.1.1), and the sequence of Hu promoter was cloned into a pSB1C3 vector (Fig.1.1.2). The sequence of the recombinant plasmid was confirmed by double enzyme digestion with EcoR I and Pst I(Fig.1.1.3) and DNA sequencing.

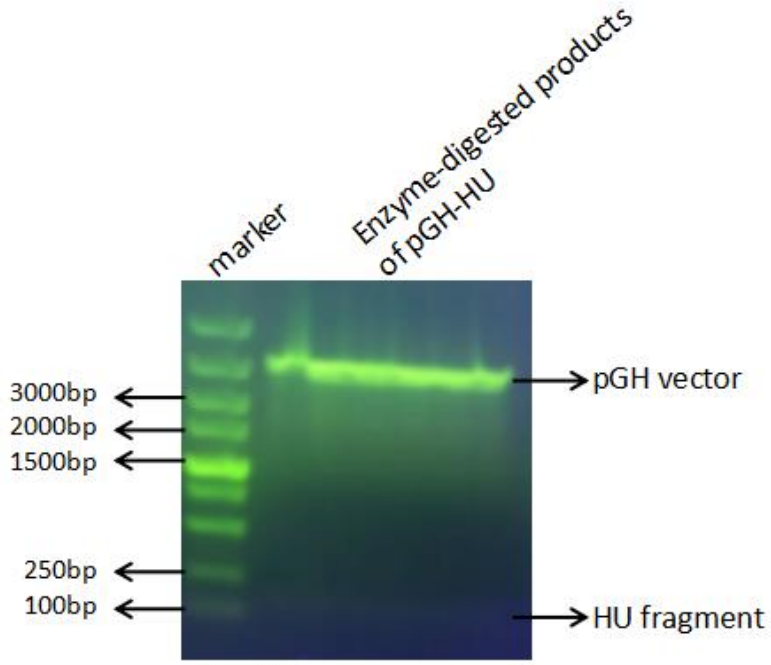

Fig.1.1.1.The plasmid pGH-HU was digested with EcoR I and Pst I, andDNA fragments were separated by agarose gel electrophoresis.

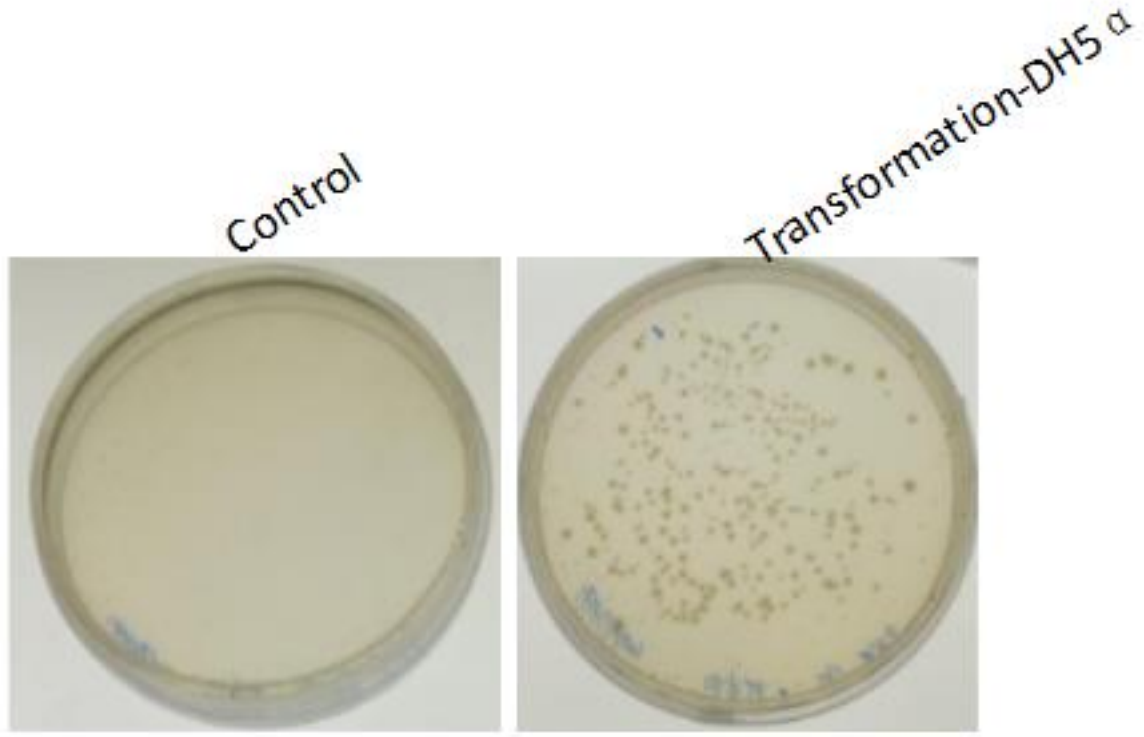

Fig.1.1.2.The HU fragment was inserted into pSB1C3 vector and the ligated products were transformed into E. *coli* DH5α competent cells (selected by Cm^r).

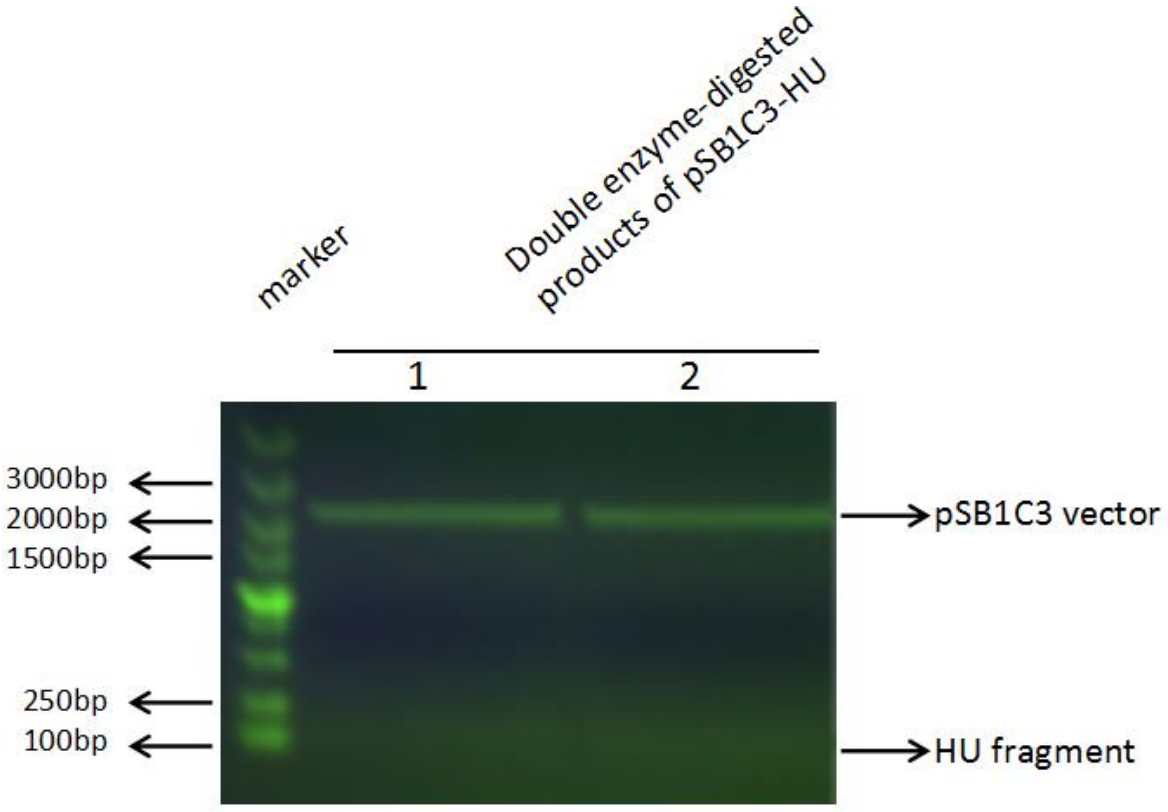

Fig.1.1.3.The recombinant plasmid (BBa_K1932000) was confirmed by double enzyme digestion with EcoR I and Pst I.
More information about BBa_K1932000 is available at http://parts.igem.org/Part:BBa_K1932000.

Sec2: BBa_K1932002

Sec2 encodes a classical SP with a predicted N-terminal signal peptide that contains a single trans-membrane region. The selected portion of this protein comprises the first 77 amino acids from the N-terminal of this putative 602 amino acid protein. This protein is significantly similar to the permease component of an ABC-type transport system, and homologues of this gene are found in B. *longum* NCC2705 (accession no. NP_695398) and DJO10A (ZP_00121339).

The signal peptide prediction was done with the tools of SingalP 4.1 Server (Fig.1.1.4) and TMpred program (Fig.1.1.5), and the results showed that it could direct the process of membrane crossing. We fused this 77 amino acid signal peptide at the N-terminal of our apoptin protein, and did the homology modeling and molecular dynamic simulation with TMHMM (Fig.1.1.6), which showed that the two domains were well separated, indicating that they should not affect the function of each other.

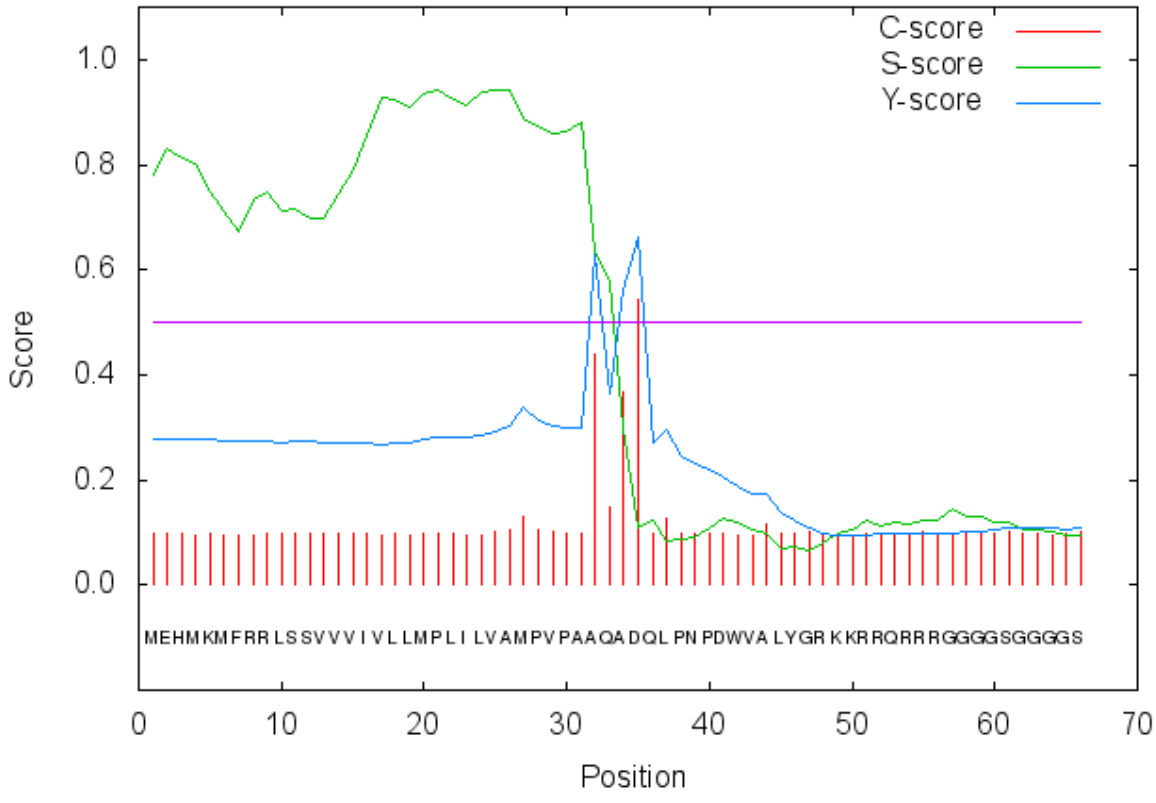

Fig.1.1.4. Prediction of Sec2 signal peptide with the SignalP 4.1 Server.

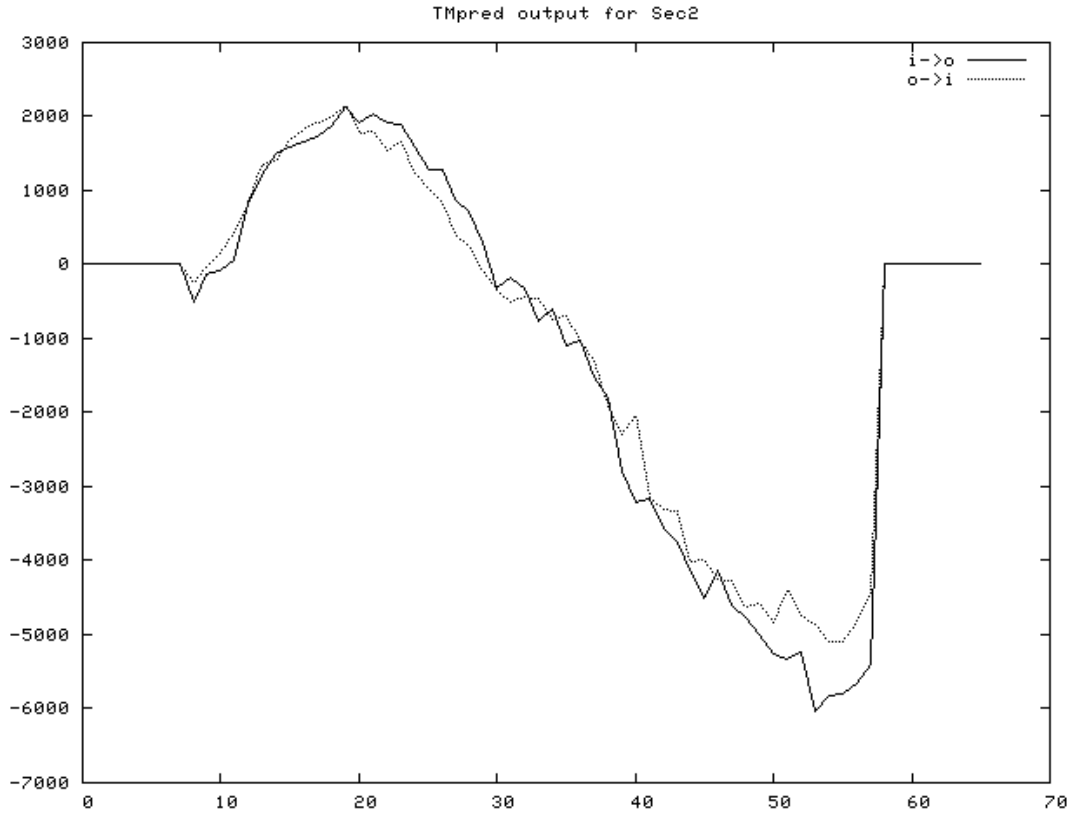

Fig.1.1.5. Analysis of Sec2 signal peptide with the TMpred.

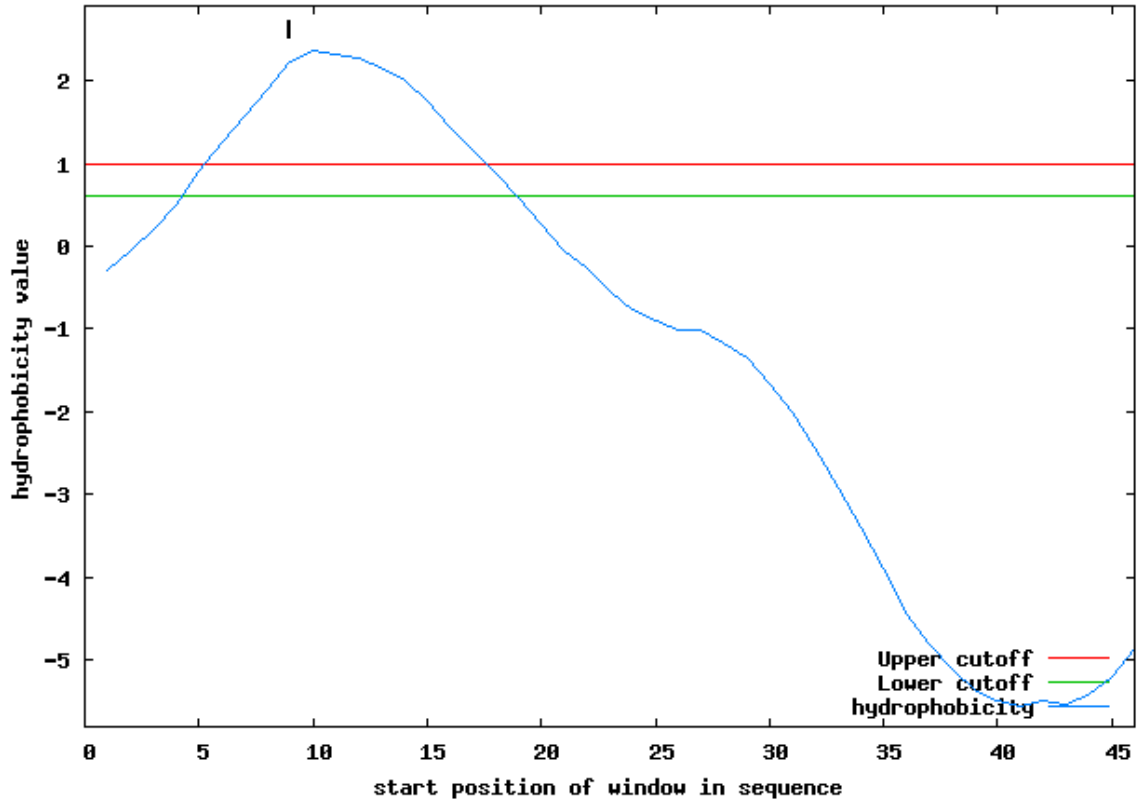

Fig.1.1.6. Analysis of Sec2 signal peptide with the TMHMM.

(More information about our modeling for Sec2 signal peptide is available at

http://2016.igem.org/Team:Jilin_China/Model.

We obtained the sequence information of Sec2 signal peptide from NCBI, and have it synthesized and cloned into a pGH vector by Generay Biotechnology. The plasmid was cut by the restriction enzyme, EcoRI and PstI (Fig.1.1.7), and the DNA fragment encoding Sec2 signal peptide was cloned into a pSB1C3 vector (Fig.1.1.8). The recombinant pSB1C3-Sec2 plasmid was confirmed by double enzyme digestion (Fig.1.1.9) and DNA sequencing.

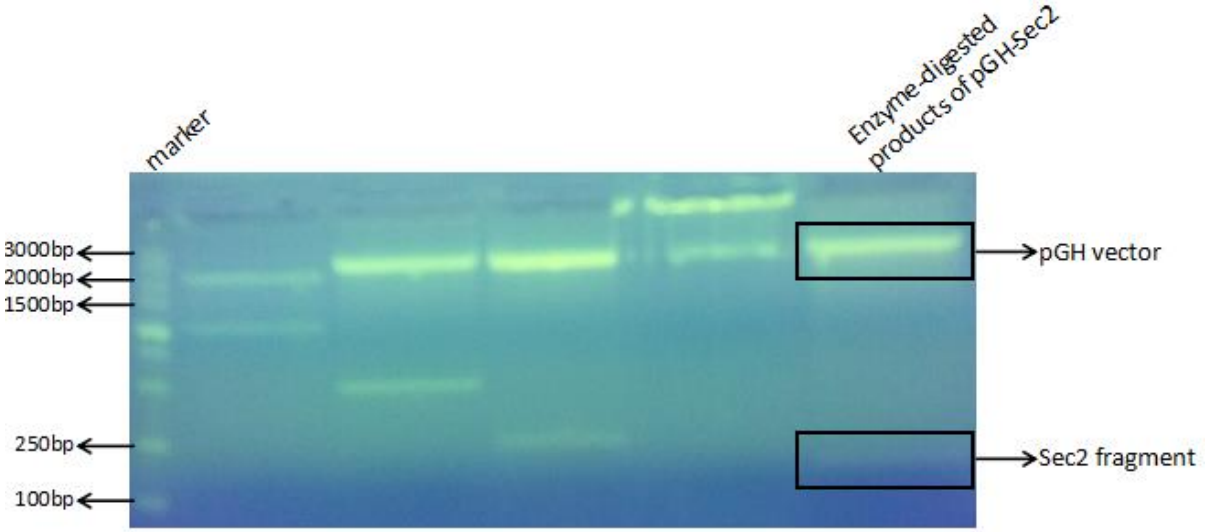

Fig.1.1.7.The plasmid pGH-Sec2 was digested with EcoRI and PstI and DNA fragments were separated by agarose gel electrophoresis

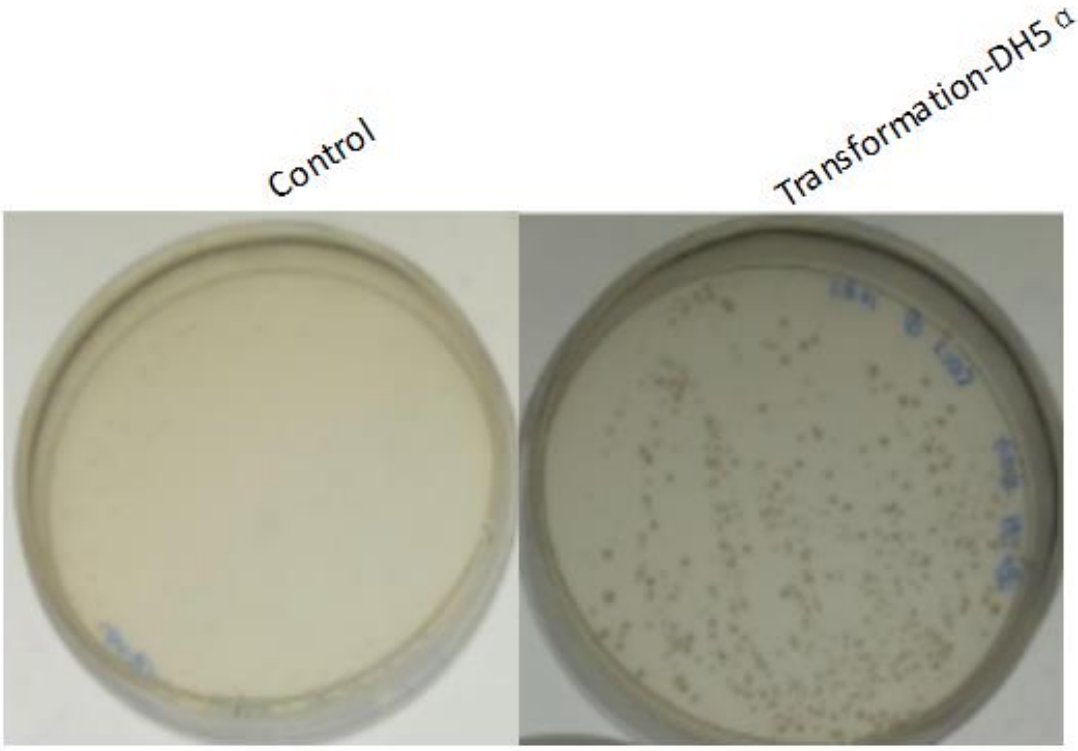

Fig.1.1.8.The Sec2 fragment was cloned into pSB1C3 vector and the connection products were

transformed into E. *coli* DH5α competent cells (selected by Cm^r).

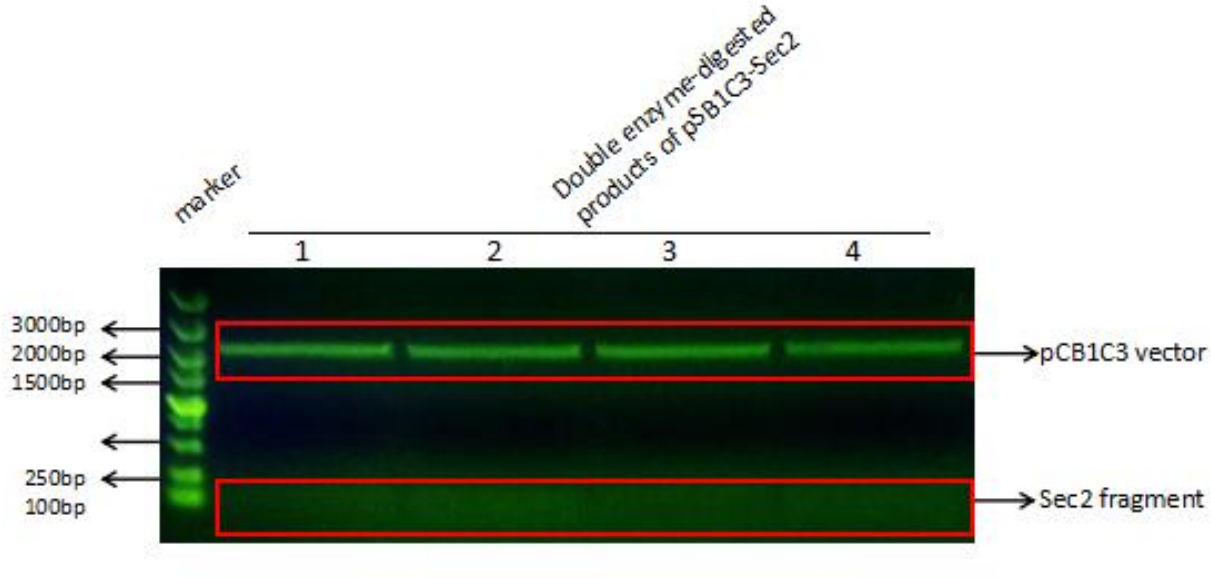

Fig.1.1.9.The recombinant plasmid (BBa_K1932002) was confirmed by double enzyme digestion.
More information about BBa_K1932002 is available at http://parts.igem.org/Part:BBa_K1932002.

Tmp1: BBa_K1932003.

TMP proteins are polypeptides that contain at least one predicted trans-membrane domain. They are identified as active Δ_{SP}Nuc fusions and designated as Tmp (trans-membrane protein). Tmp1 is the first characterized protein of TMP family. The selected portion of Tmp1 encodes the N-terminal region of a hypothetical protein and is predicted to have a C-out topology, which is a typical feature of trans-membrane proteins. Proteins homologous to Tmp1 have been found in B. *longum* NCC2705 (accession no. NP_696268) and DJO10A (ZP_00120937).

The signal peptide prediction was done with SingalP 4.1 (Fig.1.1.10) Server and TMpred program (Fig.1.1.11). And the results showed that it could direct the process of membrane crossing by cutting the former **XX** amino acids. We did the homology modeling and molecular dynamic simulation of the fused protein of TMP and apoptin with TMHMM (Fig.1.1.12), which showed that the two domains were well separated and wouldn't affect the function of each other.

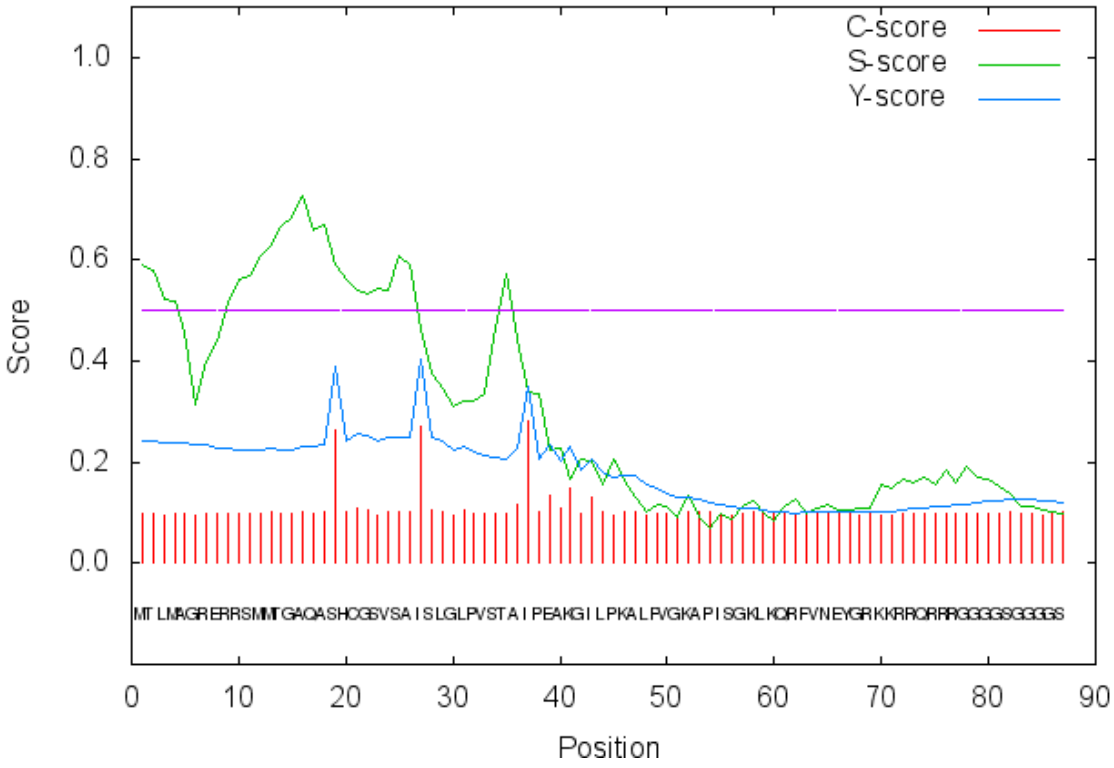

Fig.1.1.10.The Signal P 4.1 Server result for Tmp1 signal peptide sequence.

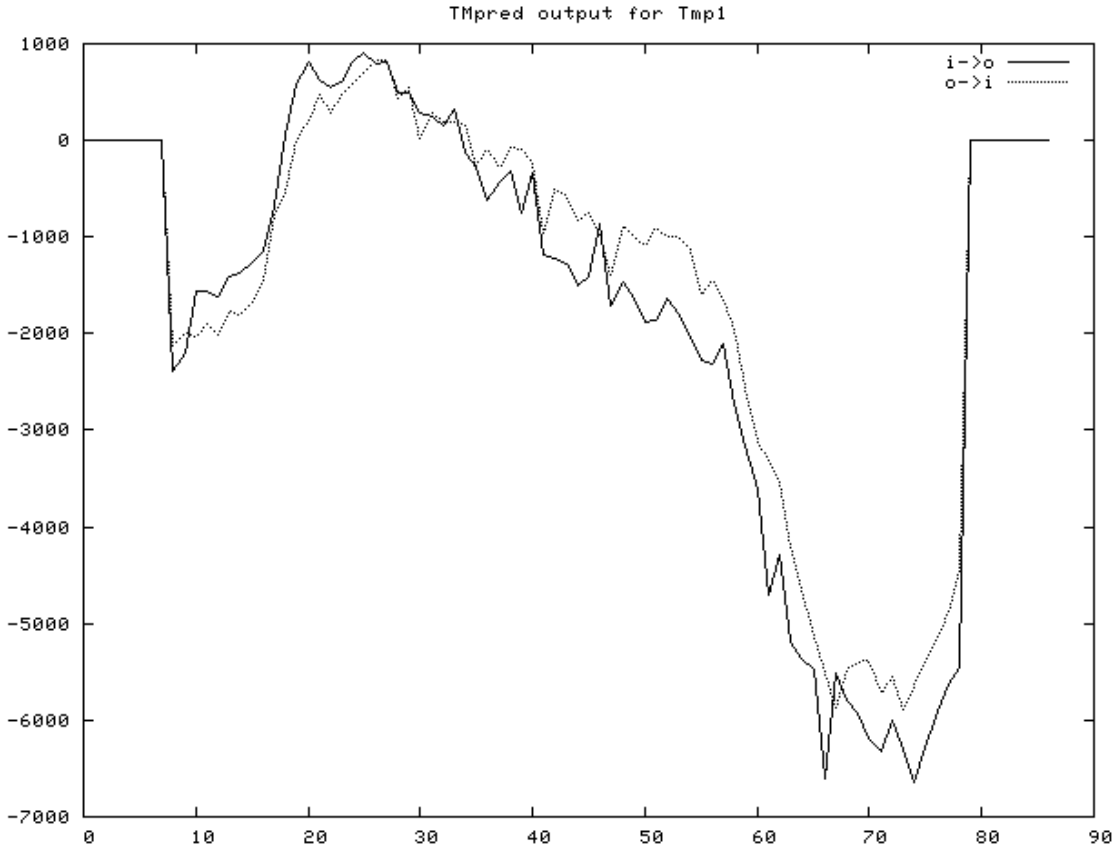

Fig.1.1.11.The TMpred result for Tmp1 signal peptide sequence.

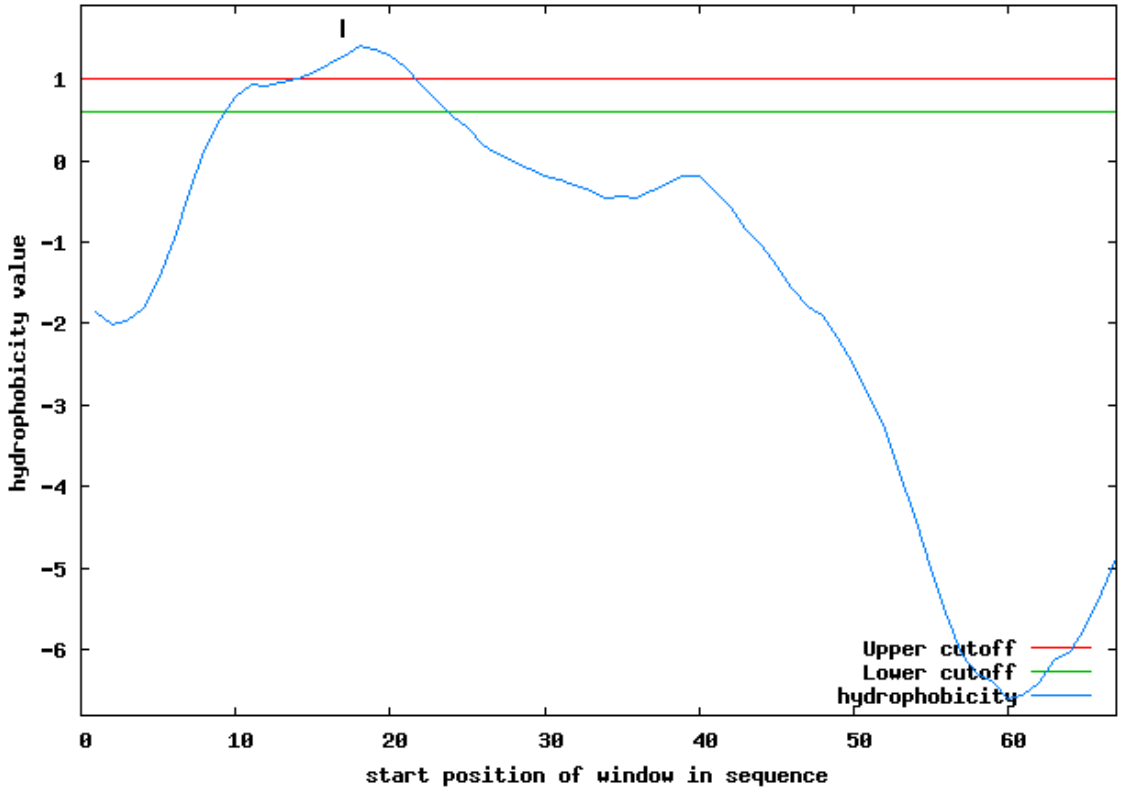

Fig.1.1.12. Analysis of Tmp1 signal peptide sequence with the TMHMM.

(More information about our modeling for Tmp1 signal peptide is available at http://2016.igem.org/Team:Jilin_China/Model.)

We retrieved the sequence information of Tmp1 signal peptide from NCBI, and have it synthesized and cloned into a pGH vector by Generay Biotechnology. The pGH-Tmp1 plasmid was cut with the restriction enzymes EcoRI and PstI (Fig.1.1.13), and the DNA fragments encoding Tmp1 was cloned into pSB1C3 vector (Fig.1.1.14). The recombinant plasmid pSB1C3-Tmp1 was confirmed by double enzyme digestion (Fig.1.1.15) and DNA sequencing.

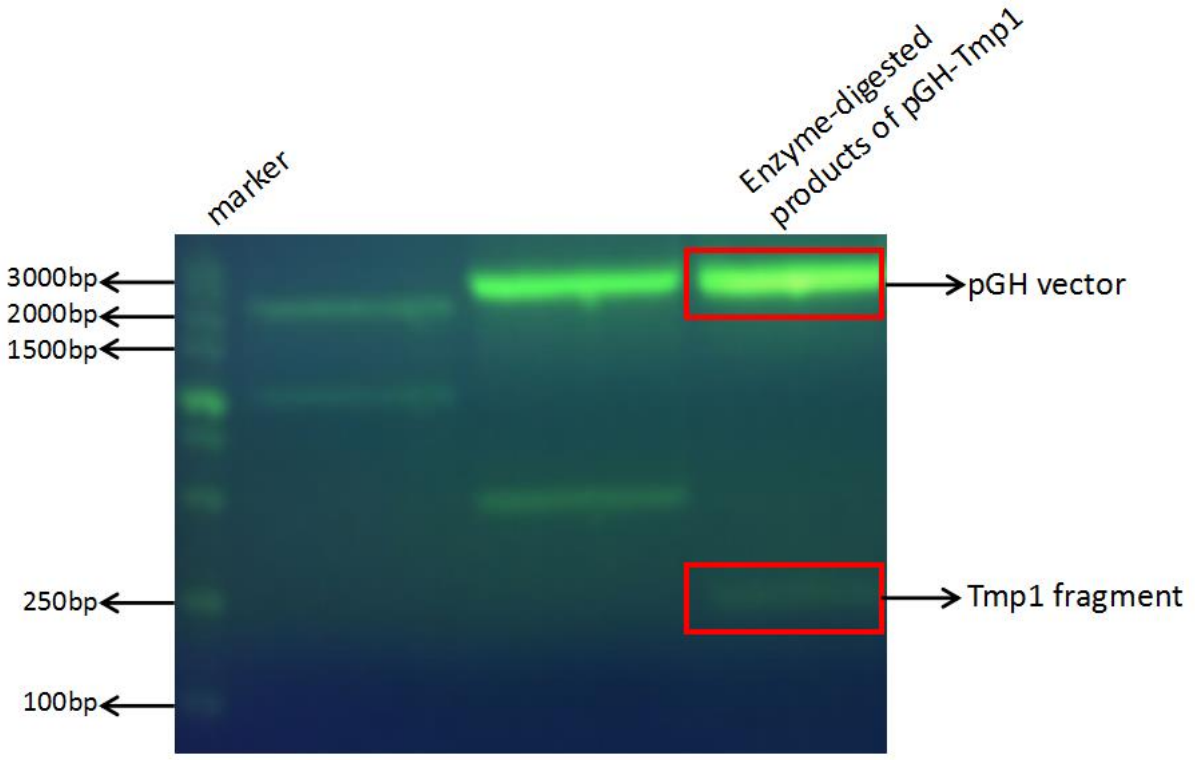

Fig.1.1.13. The plasmid pGH-Tmp1 was digested with EcoRI and PstI and the DNA fragments were separated by agarose gel electrophoresis.

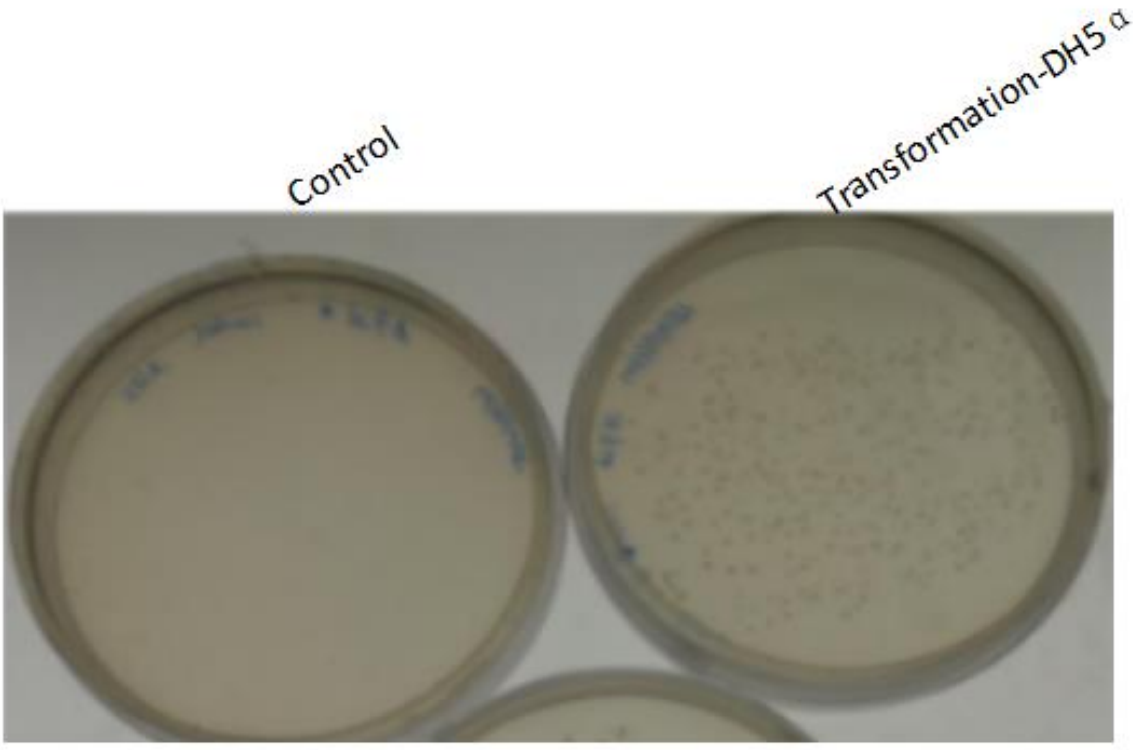

Fig.1.1.14.The Tmp1 fragment was ligated into pSB1C3 vector and the ligated products were transformed

into E. *coli* DH5α competent cells (selected by Cm^r).

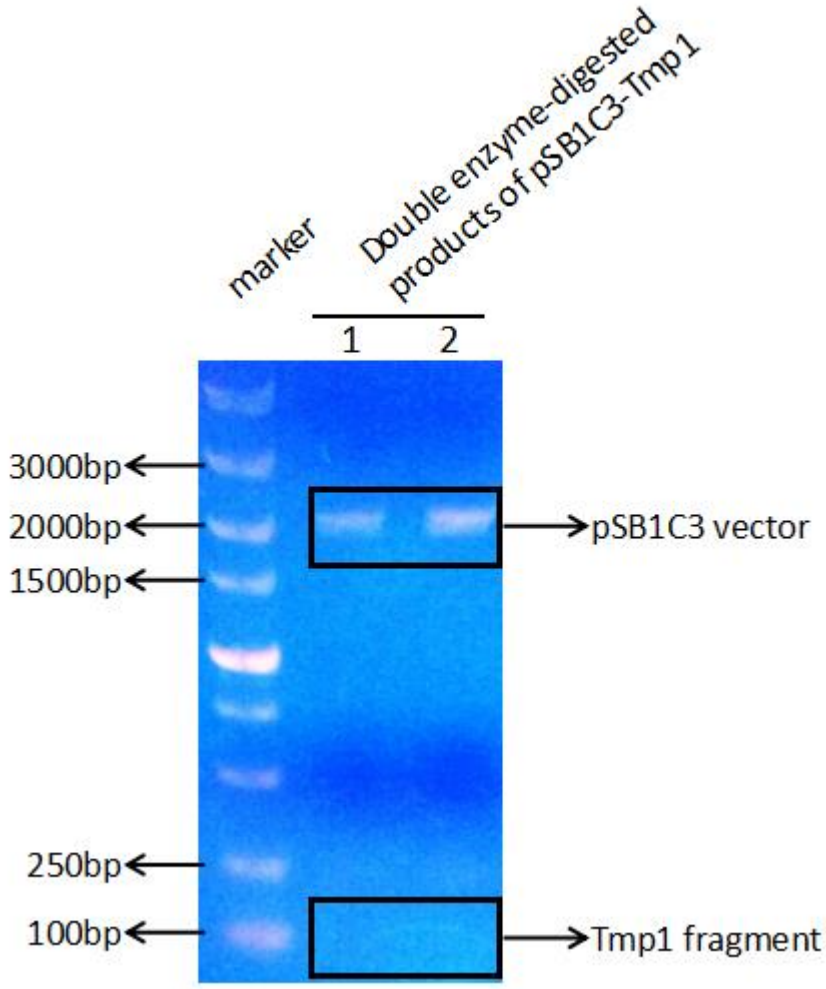

Fig.1.1.15.The recombinant plasmid (BBa_K1932003) was confirmed by double enzyme digestion.
More information about BBa_K1932003 is available at http://parts.igem.org/Part:BBa_K1932003.

TAT-apoptin: BBa_K1932004

TAT-Apoptin is a fusion protein made up of the transduction domain of HIV-1 and apoptin. Since apoptin only functions inside the cells, the peptide TAT is added to direct the transfer of the apoptin into the cell. Once transferred into the tumor cells, apoptin can induce the apoptosis of them potently.

We retrieved the sequence information of TAT-apoptin from NCBI, and have it synthesized and cloned into a pGH vector by Generay Biotechnology. The pGH-TAT-apoptin plasmid was cut with restriction enzymes EcoRI and PstI (Fig.1.1.16), and the DNA fragment encoding TAT-apoptin was cloned into a pSB1C3 vector (Fig.1.1.17). The pSB1C3-TAT-apoptin plasmid was confirmed by double enzyme digestion (Fig.1.1.18) and DNA sequencing.

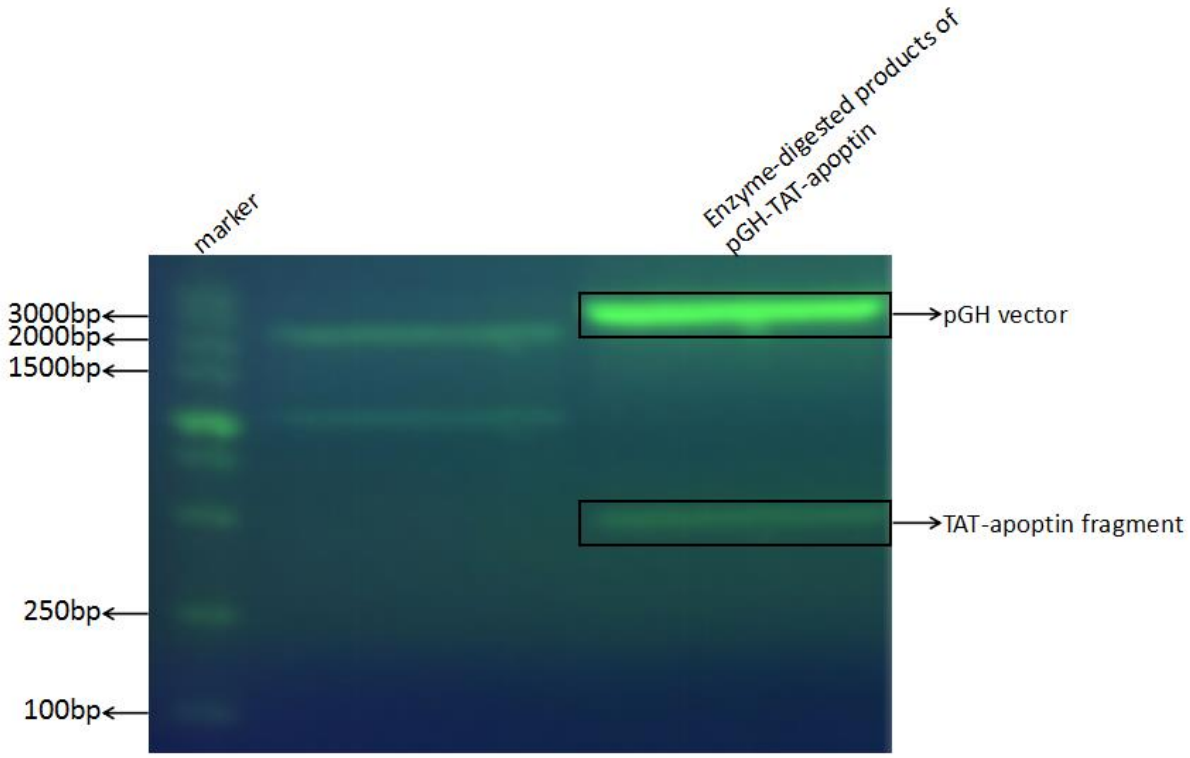

Fig.1.1.16. The plasmid pGH-TAT-apoptin was digested with EcoRI and PstI and DNA fragments were separated by agarose gel electrophoresis.

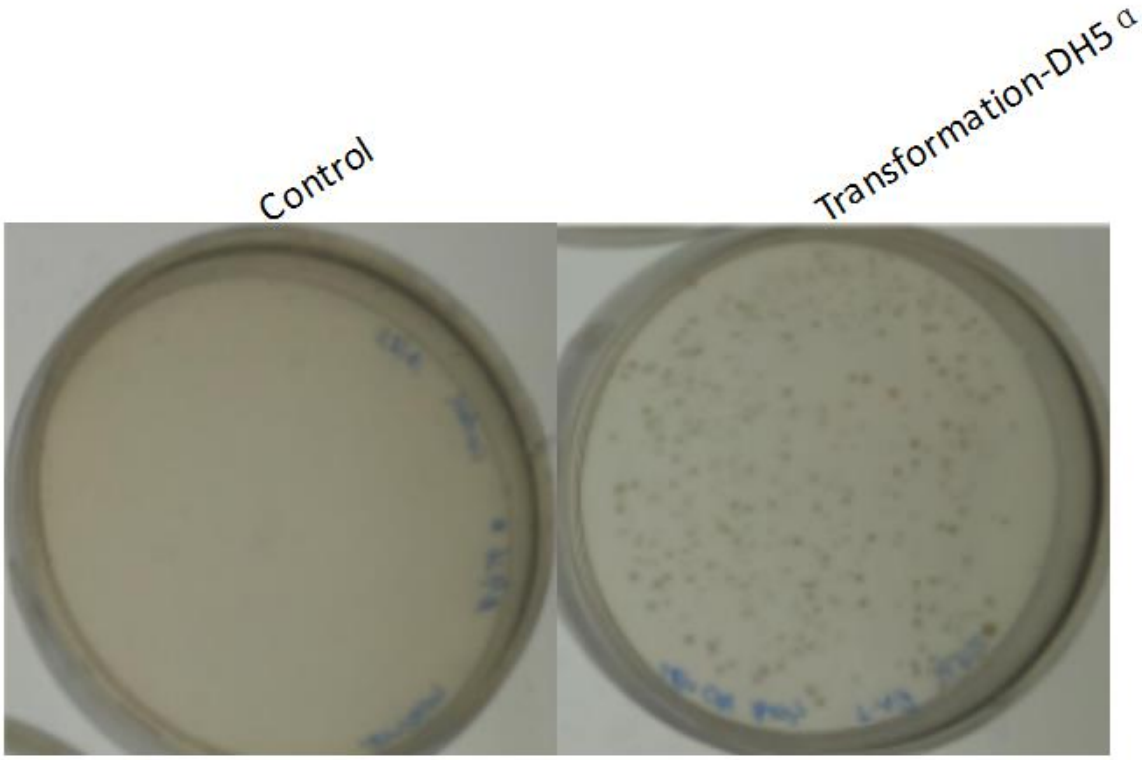

Fig.1.1.17.The TAT-apoptin fragment was ligated into pSB1C3 vector and the ligated products were transformed into E. *coli* DH5α competent cells (selected by Cm^r).

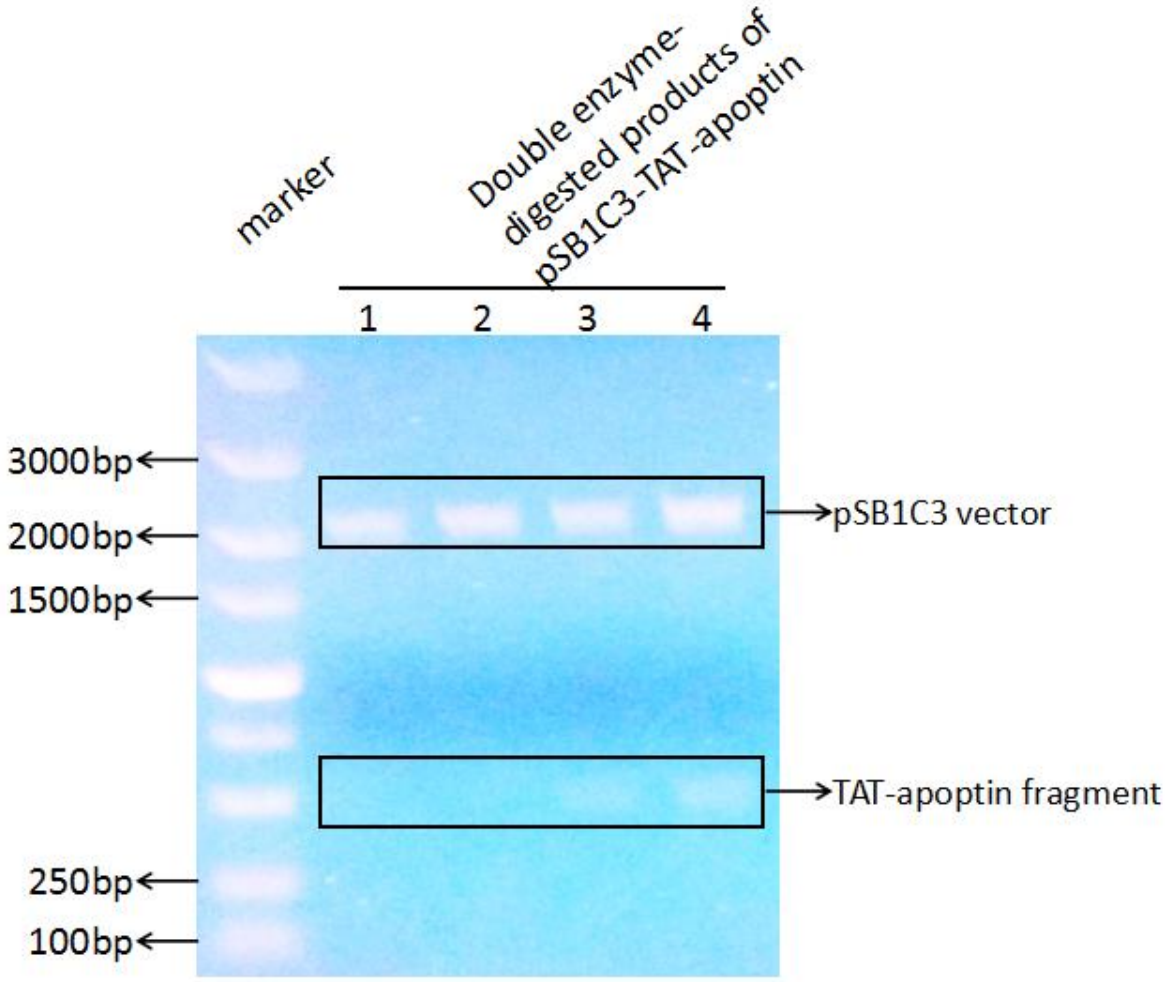

Fig.1.1.18.The pSB1C3-TAT-apoptin plasmid (BBa_K1932004) was confirmed by double enzyme digestion.

More information about BBa_K1932004 is available at http://parts.igem.org/Part:BBa_K1932004.

PMB1: BBa_K1932001

Part BBa_K1932001 was originally cloned from the plasmid of Bifidobacterium that contains a sequence of ori and two sequences of orf.（The plasmid had a G + C content of 62.0%, and contained two open reading frames, orf1 and orf2, likely arranged in an operon.）This sequence is essential for the shuttling of the plasmid from E. coli to Bifidobacterium.

We retrieved the sequence information of PMB1 from NCBI, and have it synthesized and cloned into a pGH vector by Generay Biotechnology. The pGH-PMB1 plasmid was cut with the restriction enzymes EcoRI and PstI (Fig.1.1.18), and the DNA fragment encoding PMB1 was cloned into a pSB1C3 vector (Fig.1.1.19).

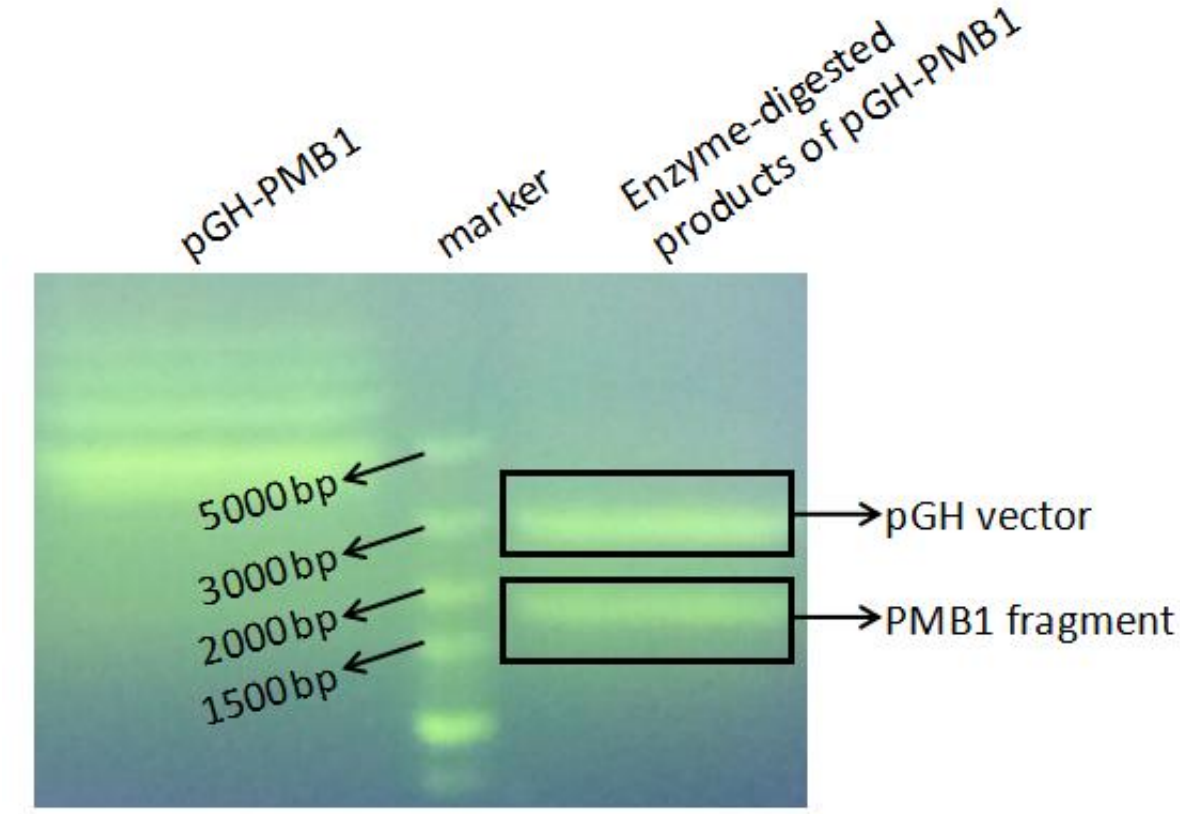

Fig.1.1.18.The DNA fragments were separated by agarose gel electrophoresis after digesting the plasmid pGH-PMB1 with EcoRI and PstI.

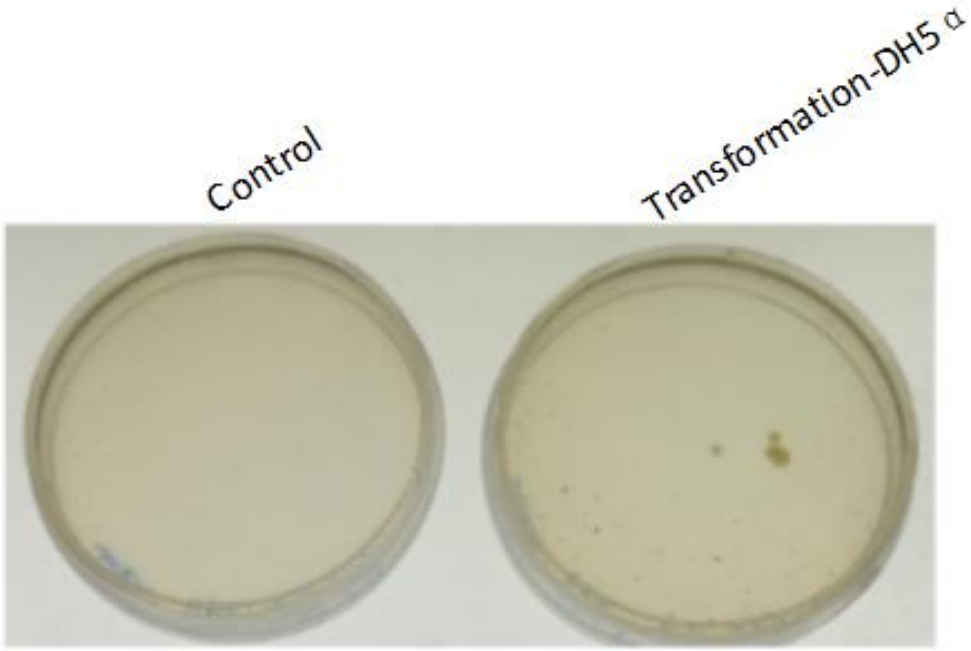

Fig.1.1.19.The PMB1 fragment was ligated into pSB1C3 vector and the ligated products were transformed into E. Coli DH5α competent cells (selected by Cm^r).

Fig.1.1.20.The recombinant plasmid (BBa_K1932001) was confirmed by double enzyme digestion.
More information about BBa_K1932000 is available at http://parts.igem.org/Part:BBa_K1932000.

Composite parts:

PMB1-HU-TAT-apoptin: BBa_K1932005

This device is designed for robust expression of the TAT-apoptin. Among the subparts, BBa_K1932000 encodes a strong promoter to regulate the expression of TAT-apoptin in Bifidobacterium. BBa_K1932001 is included in this device to increase the stability of the device in Bifidobacterium. BBa_K1932004 encodes TAT-apoptin, which acts as the effector protein to kill the cancer cells.

We designed this device have it synthesized and cloned into a pGH vector by Generay Biotechnology. The pGH-PMB1-HU-TAT-apoptin plasmid was cut with restriction enzymes EcoRI and PstI (Fig.1.2.1), and the DNA fragment encoding PMB1-HU-TAT-apoptin was cloned it into pSB1C3 vector (Fig.1.2.2).

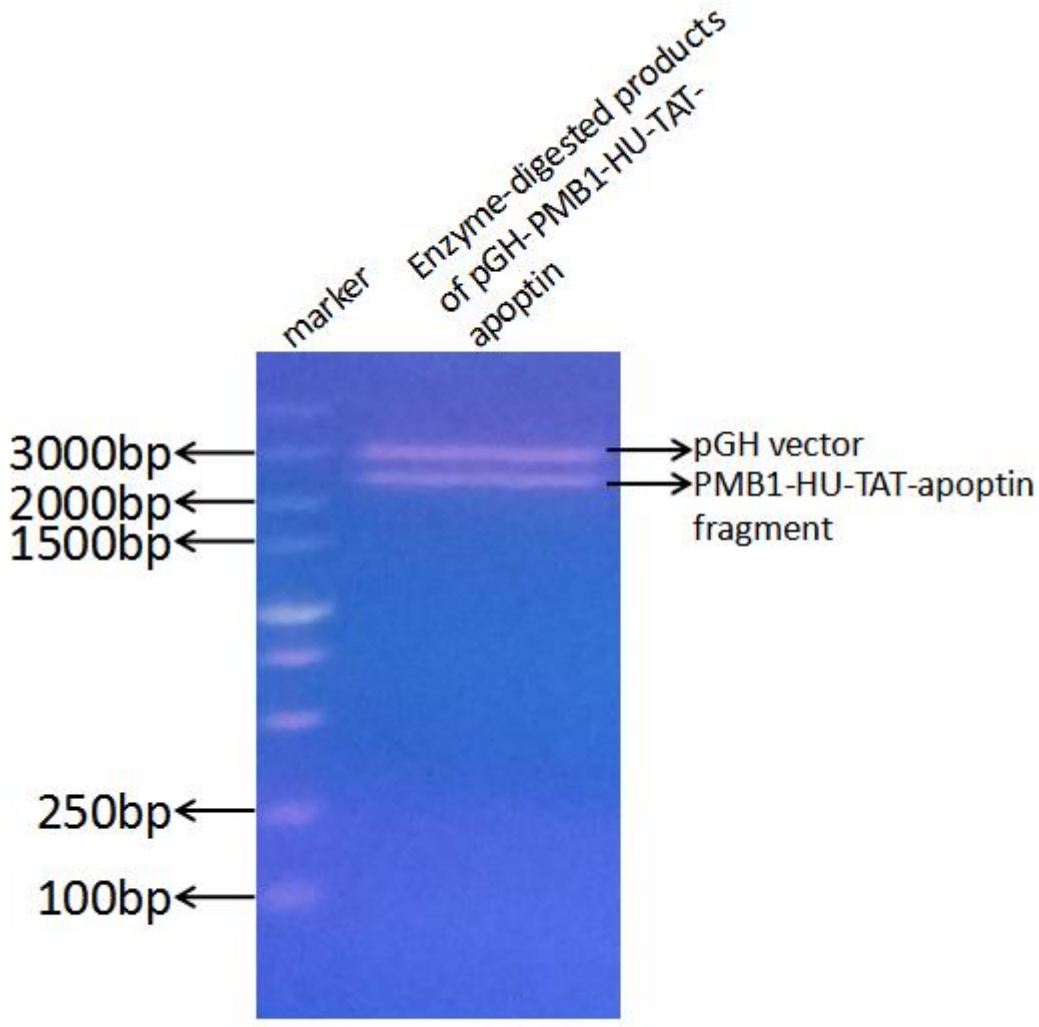

Fig.1.2.1.The DNA fragments were separated by agarose gel electrophoresis after the plasmid pGH-PMB1-HU-TAT-apoptin was digested with EcoRI and PstI.

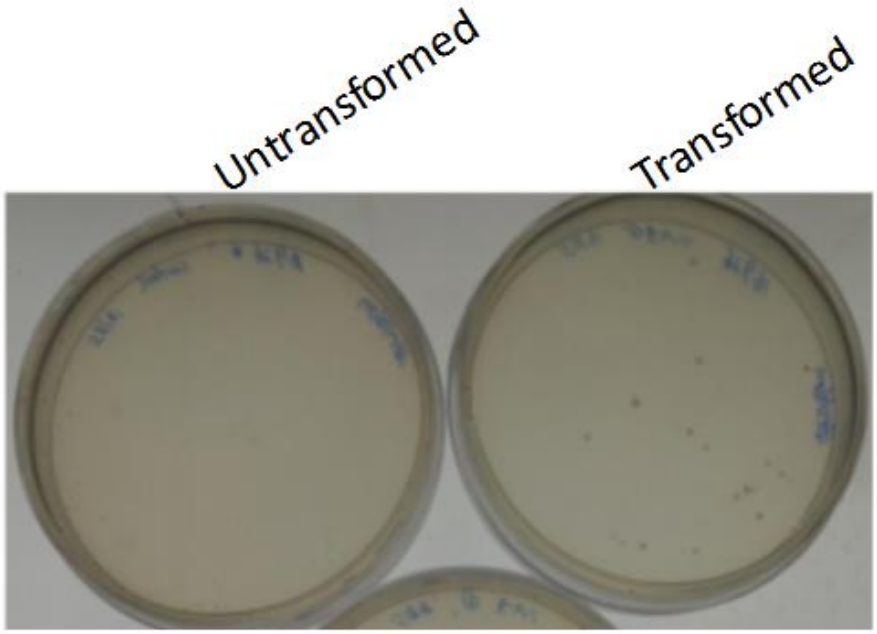

Fig.1.2.2.The PMB1-HU-TAT-apoptin fragment was inserted into pSB1C3 vector and the connection products were transformed into E. *coli* DH5α competent cells (selected by Cm^r).
More information about BBa_K1932005:
http://parts.igem.org/Part:BBa_K1932005

PMB1-HU-Sec2-TAT-apoptin: BBa_K1932006

This device consists of BBa_K1932000, BBa_K1932001, BBa_K1932002 and BBa_K1932004. This device is constructed to express TAT-Apoptin fused with sec2 signal peptide.

We designed this device to express TAT-Apoptin with a sec2 peptide to increase the secretion of the protein. Among the subparts, BBa_K1932000 is a strong promoter to regulate the expression of TAT-apoptin in Bifidobacterium. BBa_K1932001 is included to enhance the stability of the device in Bifidobacterium. BBa_K1932002 encodes the signal peptide sec2, which facilitates the export of the protein from Bididobacterium. BBa_K1932004 encodes the TAT-apoptin fusion protein, which can induce the apoptosis of cancer cells.

To simulate the structure of this protein, we used the Phyre2 web portal for protein modeling and Hyperchem 8.0 for Molecular Dynamic Simulation (Fig.1.2.3).

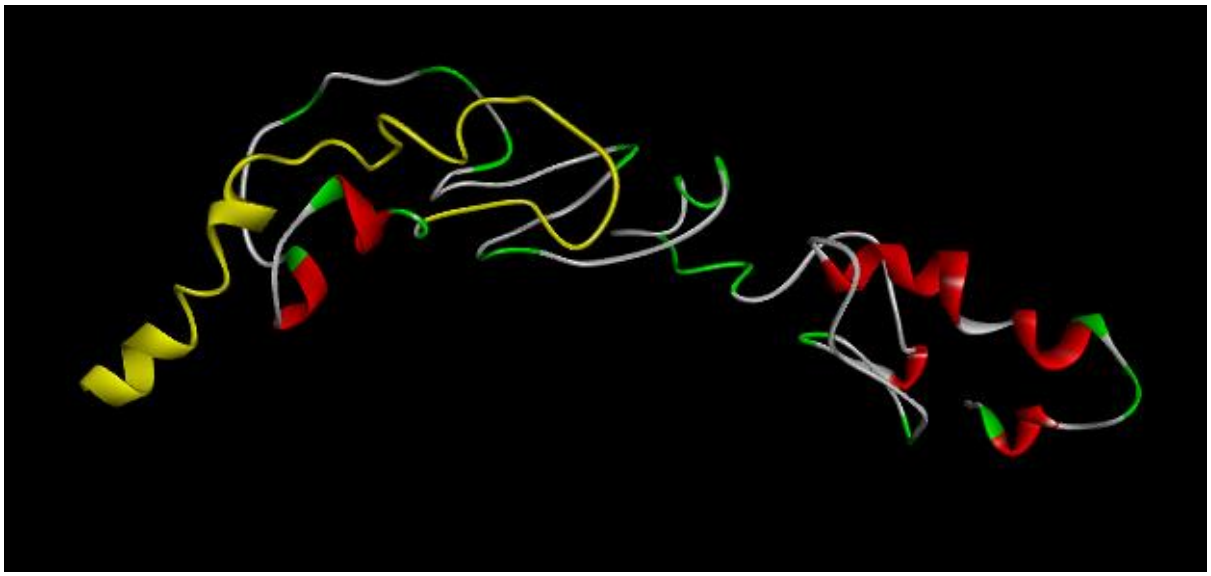

Fig.1.2.3.The predicted structures for Sec2-TAT-apoptin. Sec2 signal peptide is highlighted in yellow. (More information about our modeling for this protein is available at http://2016.igem.org/Team:Jilin_China/Model.)

We have this device synthesized and cloned into a pGH vector by Generay Biotechnology. The plasmid pGH-PMB1-HU-Sec2-TAT-apoptin was cut with the restriction enzymes EcoRI and PstI (Fig.1.2.4), and the DNA fragment encoding PMB1-HU-SEC2-TAT-apoptin was cloned it into a pSB1C3 vector (Fig.1.2.5). The recombinant plasmid pSB1C3-PMB1-HU-Sec2-TAT-apoptin was confirmed by a double-enzyme digestion (Fig.1.2.6) and DNA sequencing.

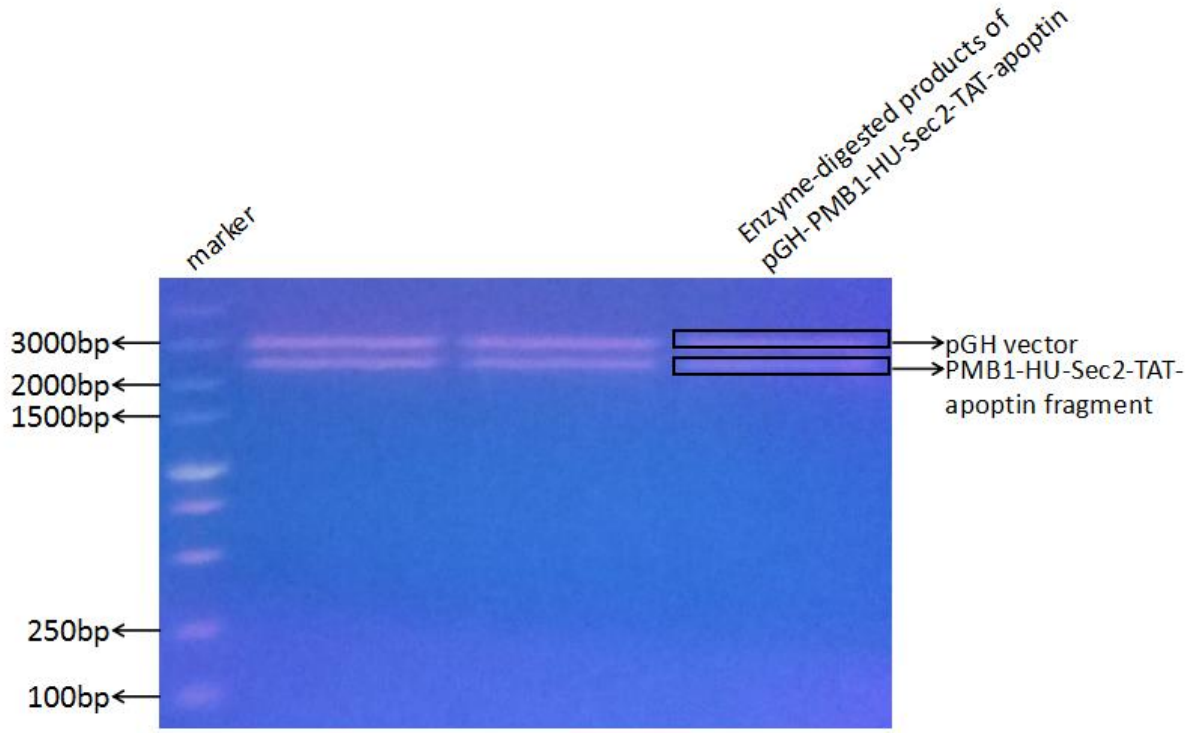

Fig.1.2.4.The DNA fragments were separated by agarose gel electrophoresis after the plasmid pGH-PMB1-HU-Sec2-TAT-apoptin was digested with EcoRI and PstI.

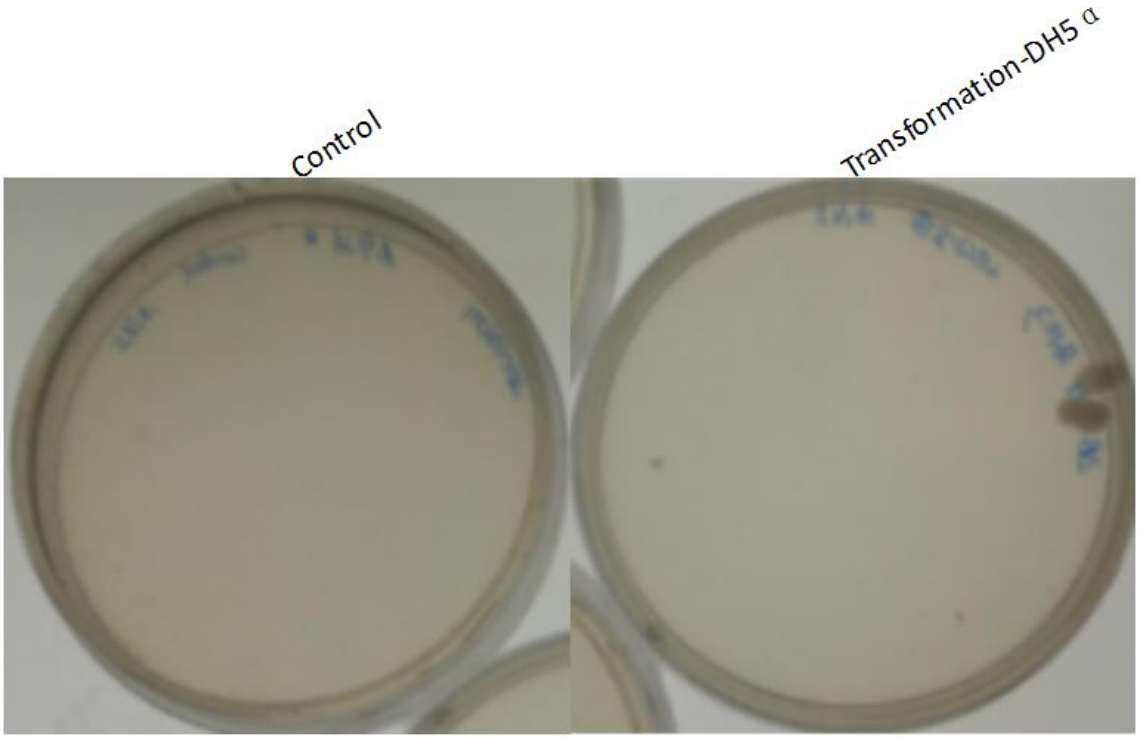

Fig.1.2.5.The PMB1-HU-Sec2-TAT-apoptin fragment was ligated into pSB1C3 vector and the ligated products were transformed into E. *coli* DH5α competent cells (selected by Cm^r).

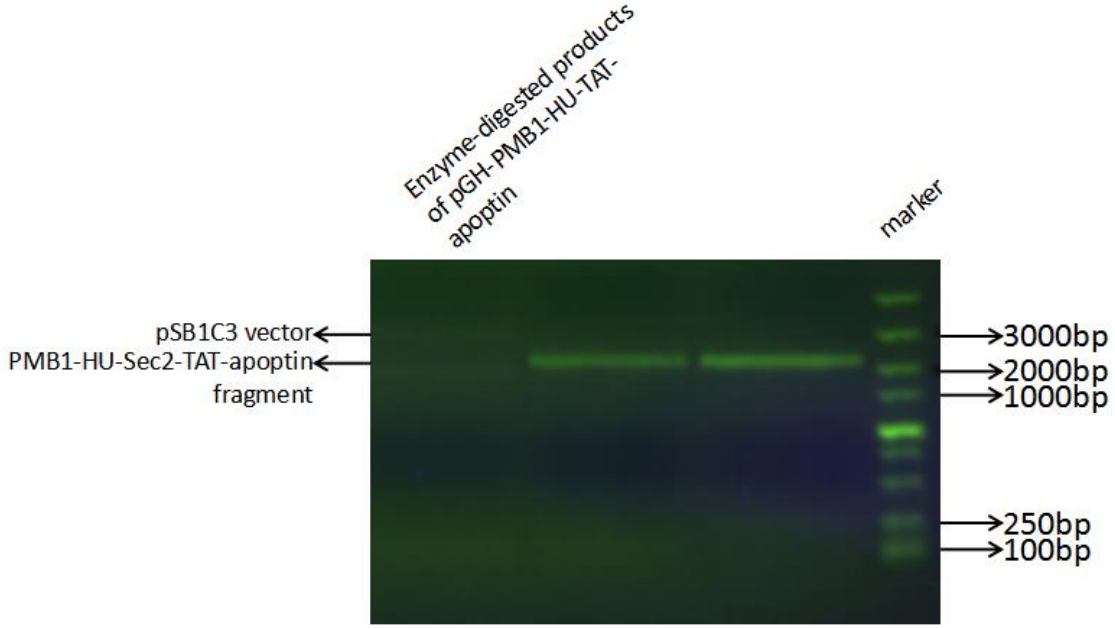

Fig.1.2.6.The recombinant plasmid (BBa_K1932006) was confirmed by double enzyme digestion.
More information about BBa_K1932006 is available at http://parts.igem.org/Part:BBa_K1932006.

PMB1-HU-Tmp1-TAT-apoptin: BBa_K1932007

This device consists of BBa_1932000, BBa_1932001, BBa_1932003 and BBa_1932004. It is constructed for the expression of TAT-apoptin fused with Tmp1.

BBa_K1932007 is constructed to express the fusion protein TAT-apoptin with a signal peptide tmp1 is to increase the secretion of TAT-apoptin. Among the subparts, BBa_1932000 is included as a promoter to regulate the expression of TAT-apoptin in Bifidobacterium. BBa_1932001 is included into this device to increase the stability of this plasmid in Bifidobacterium. BBa_1932003 encodes the signal peptide, tmp1, which can direct the export of the protein from Bididobacterium. BBa_1932004 encodes TAT-apoptin, which acts as the effector protein to kill the cancer cells.

To simulate the structure of this protein, we used the Phyre2 web portal for protein modeling and Hyperchem 8.0 for Molecular Dynamic Simulation (Fig.1.2.7).

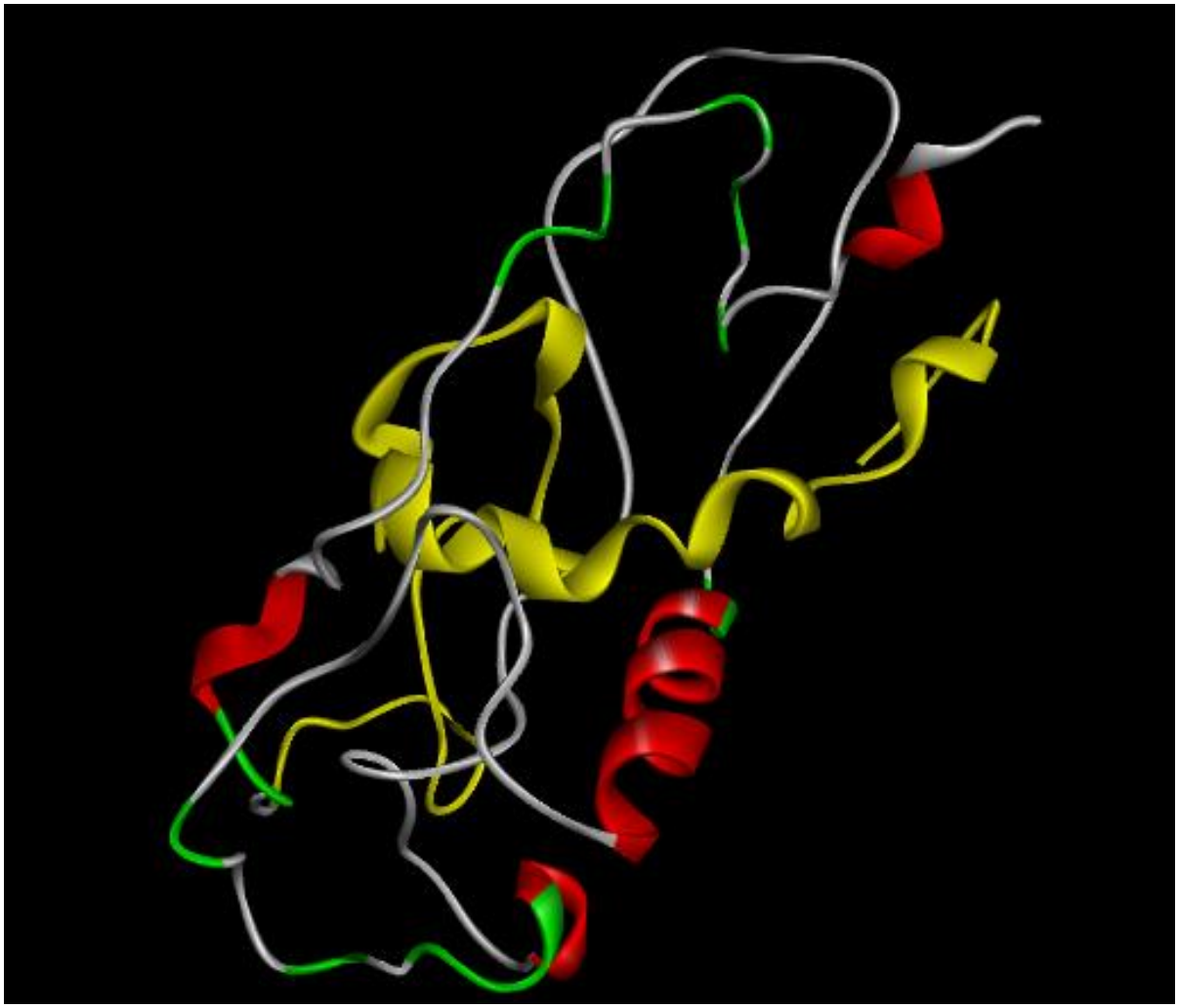

Fig.1.2.7.The predicted structures for Tmp1-TAT-apoptin. The Tmp1 signal peptide is highlighted in yellow.

We have this device synthesized and cloned into a pGH vector by Generay Biotechnology. The plasmid pGH-PMB1-HU-Tmp1-TAT-apoptin was cut with the restriction enzymes EcoRI and PstI (Fig.1.2.8), and the DNA fragment encoding PMB1-HU-Tmp1-TAT-apoptin was cloned it into a pSB1C3 vector (Fig.1.2.9). The recombinant plasmid pSB1C3-PMB1-HU-Tmp1-TAT-apoptin was confirmed by a double-enzyme digestion (Fig.1.2.10) and DNA sequencing.

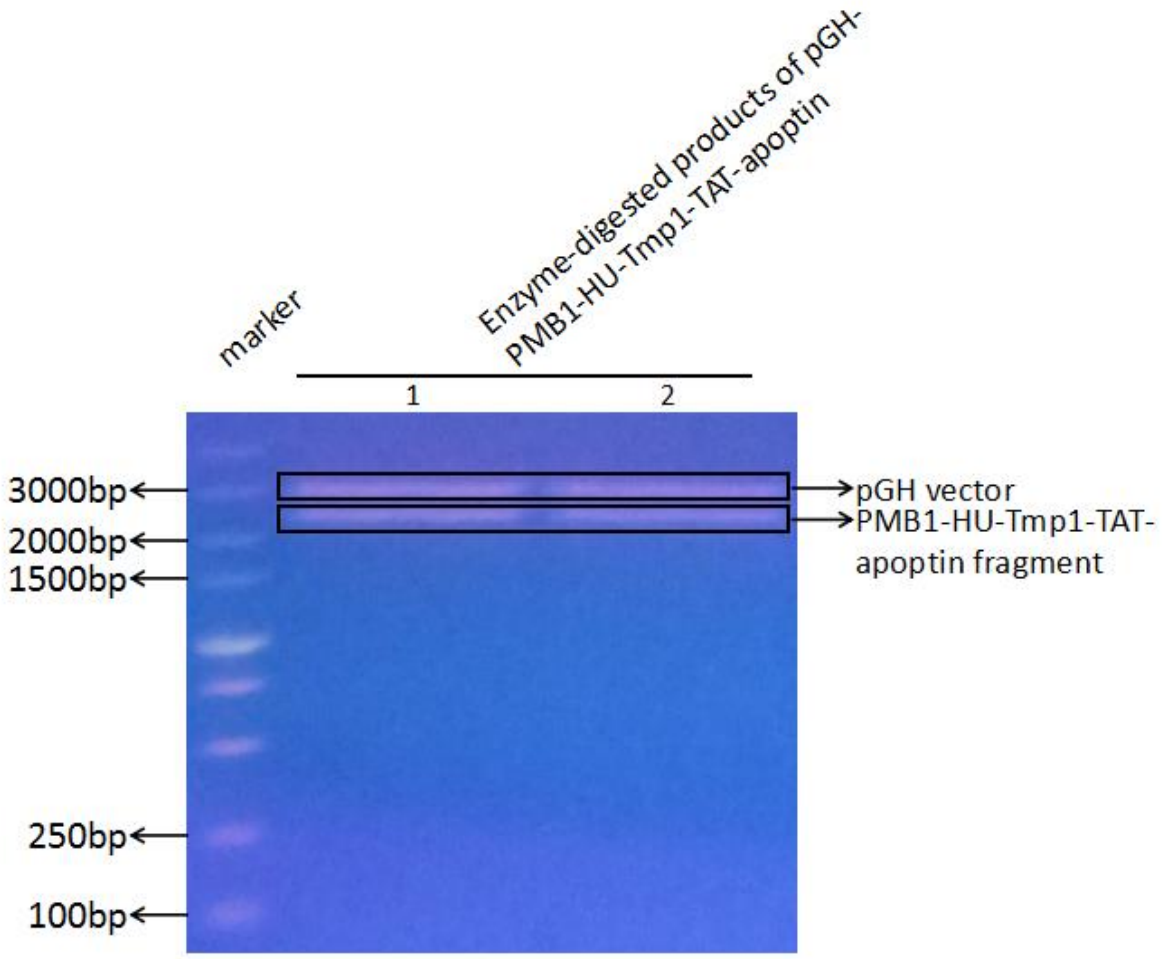

Fig.1.2.8The DNA fragments were separated by agarose gel electrophoresis after the plasmid pGH-PMB1-HU-Tmp1-TAT-apoptin was digested with EcoRI and PstI.

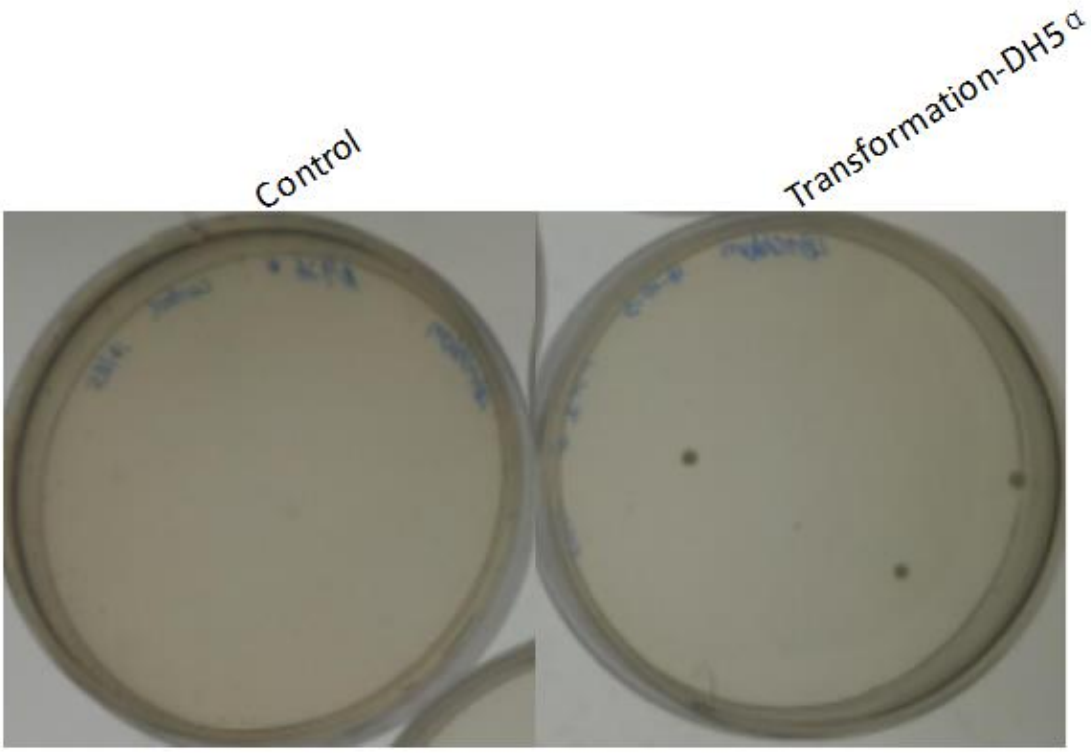

Fig.1.2.9.The PMB1-HU-Tmp1-TAT-apoptin fragment was ligated into pSB1C3 vector and the ligated products were transformed into E. *coli* DH5α competent cells (selected by Cm^r).

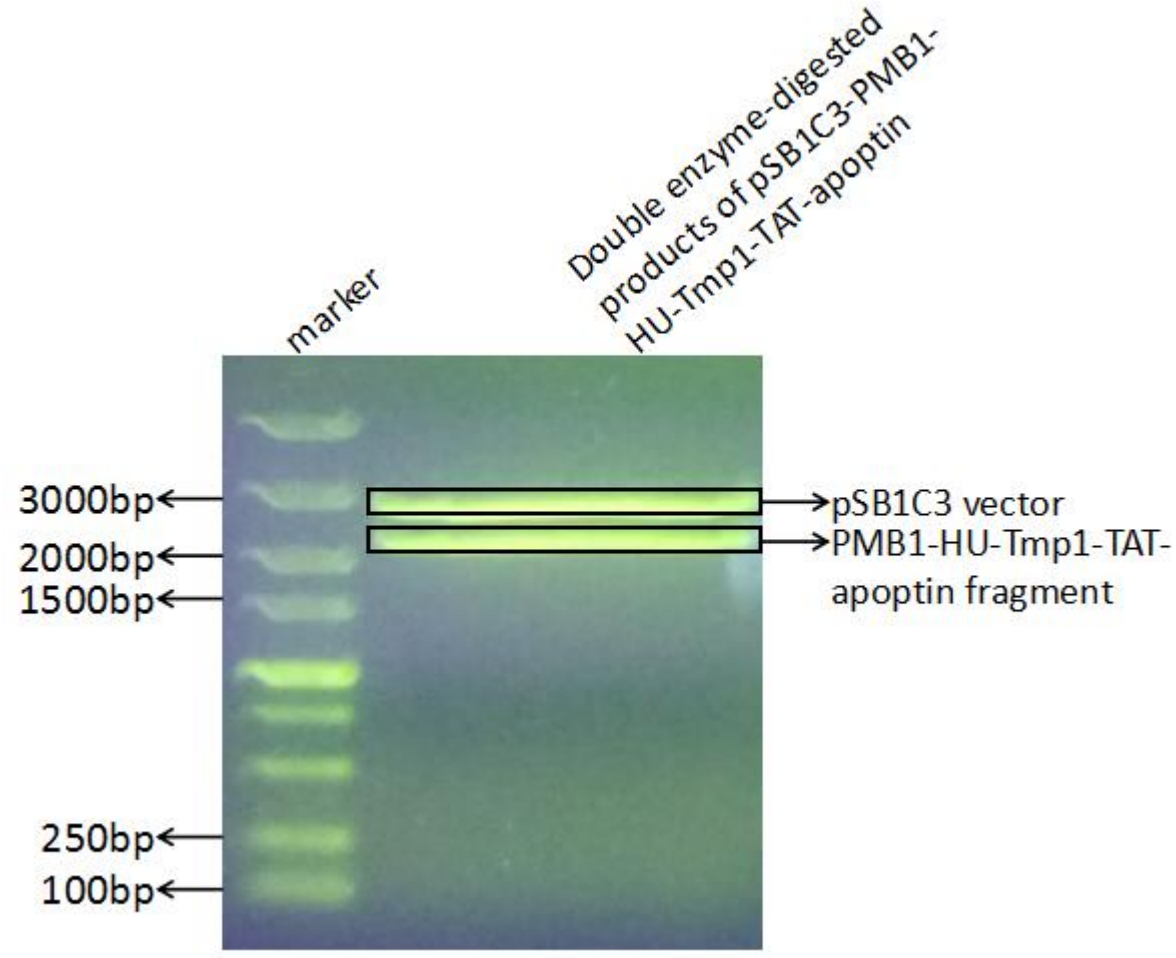

Fig.1.2.10.The recombinant plasmid (BBa_K1932007) was confirmed by double enzyme digestion. More information about BBa_K1932007 is available at http://parts.igem.org/Part:BBa_K1932007.

Extended work:

For diagnosing solid tumor, we tried to use RFP as a biomarker in our expression system, and UESTC-China helped us construct a plasmid, pSB1C3-HU-RFP (Fig.1.3).

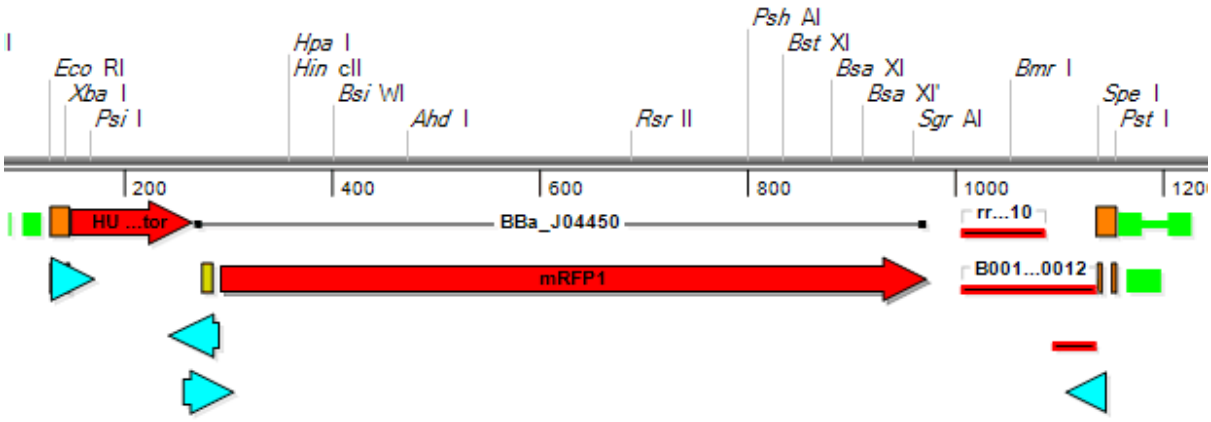

Fig.1.3.The plasmid constructed by UESTC-China.

References:

[1] Takeuchi, A., Matsumura, H., & Kano, Y. (2002). Cloning and expression in Escherichia coli of a gene, hup, encoding the histone-like protein HU of Bifidobacterium longum. *Bioscience, biotechnology, and biochemistry*, *66*(3), 598-603.

[2] Nakamura, T., Sasaki, T., Fujimori, M., Yazawa, K., Kano, Y., Amano, J., & Taniguchi, S. I. (2002). Cloned cytosine deaminase gene expression of Bifidobacterium longum and application to enzyme/pro-drug therapy of hypoxic solid tumors. *Bioscience, biotechnology, and biochemistry*, *66*(11), 2362-2366.

[3] Klijn, A., Moine, D., Delley, M., Mercenier, A., Arigoni, F., & Pridmore, R. D. (2006). Construction of a reporter vector for the analysis of Bifidobacterium longum promoters. *Applied and environmental microbiology*, 72(11), 7401-7405.

[4] Hamaji, Y., Fujimori, M., Sasaki, T., Matsuhashi, H., Matsui-Seki, K., Shimatani-Shibata, Y., ... & TANIGUCHI, S. I. (2007). Strong enhancement of recombinant cytosine deaminase activity in Bifidobacterium longum for tumor-targeting enzyme/prodrug therapy. *Bioscience, biotechnology, and biochemistry*, *71*(4), 874-883.

[5] MacConaill, L. E., Fitzgerald, G. F., & van Sinderen, D. (2003). Investigation of protein export in Bifidobacterium breve UCC2003. *Applied and environmental microbiology*, *69*(12), 6994-7001.

[6] Poquet, I., Ehrlich, S. D., & Gruss, A. (1998). An export-specific reporter designed for gram-positive bacteria: application to Lactococcus lactis. *Journal of bacteriology*, *180*(7), 1904-1912.

[7] Schell, M. A., Karmirantzou, M., Snel, B., Vilanova, D., Berger, B., Pessi, G., ... & Pridmore, R. D. (2002). The genome sequence of Bifidobacterium longum reflects its adaptation to the human gastrointestinal tract. *Proceedings of the National Academy of Sciences*, *99*(22), 14422-14427.

[8] MacConaill, L. E., Fitzgerald, G. F., & van Sinderen, D. (2003). Investigation of protein export in Bifidobacterium breve UCC2003. *Applied and environmental microbiology*, *69*(12), 6994-7001.

[9] Poquet, I., Ehrlich, S. D., & Gruss, A. (1998). An export-specific reporter designed for gram-positive bacteria: application to Lactococcus lactis. *Journal of bacteriology*, *180*(7), 1904-1912.

[10] Schell, M. A., Karmirantzou, M., Snel, B., Vilanova, D., Berger, B., Pessi, G., ... & Pridmore, R. D. (2002). The genome sequence of Bifidobacterium longum reflects its adaptation to the human gastrointestinal tract. *Proceedings of the National Academy of Sciences*, *99*(22), 14422-14427.

[11] Danen-Van Oorschot, A. A. A. M., Fischer, D. F., Grimbergen, J. E., Klein, B., Zhuang, S. M., Falkenburg, J. H. F., ... & Noteborn, M. H. M. (1997). Apoptin induces apoptosis in human transformed and malignant cells but not in normal cells. *Proceedings of the National Academy of Sciences*, *94*(11), 5843-5847.

[12] Li, J., Wang, H., Ma, Z., Fan, W., Li, Y., Han, B., ... & Wang, J. (2012). TAT-Apoptin induces apoptosis in the human bladder cancer EJ cell line and regulates Bax, Bcl-2, caspase-3 and survivin expression. *Exp Ther Med*, *3*(6), 1033-8.

[13] Ma, J. L., Han, S. X., Zhao, J., Zhang, D., Wang, L., Li, Y. D., & Zhu, Q. (2012). Systemic delivery of lentivirus-mediated secretable TAT-apoptin eradicates hepatocellular carcinoma xenografts in nude mice. *International journal of oncology*, *41*(3), 1013-1020.

[14] Zhou, S., Zhang, M., & Wang, J. (2011). Tumor-targeted delivery of TAT-Apoptin fusion gene using Escherichia coli Nissle 1917 to colorectal cancer. *Medical hypotheses*, *76*(4), 533-534.

[15] Guelen, L., Paterson, H., Gäken, J., Meyers, M., Farzaneh, F., & Tavassoli, M. (2004). TAT-apoptin is efficiently delivered and induces apoptosis in cancer cells. *Oncogene*, *23*(5), 1153-1165.

[16] Rossi, M., Brigidi, P., y Rodriguez, A. G. V., & Matteuzzi, D. (1996). Characterization of the plasmid pMB1 from Bifidobacterium longum and its use for shuttle vector construction. *Research in microbiology*, *147(3)*, 133-143.
[17] Matteuzzi, D., Brigidi, P., Rossi, M., & Di, D. (1990). Characterization and molecular cloning of Bifidobacterium longum cryptic plasmid pMB1. *Letters in applied microbiology, 11(4)*, 220-223.
[18] Xu, Y. F., Zhu, L. P., Hu, B., Fu, G. F., Zhang, H. Y., Wang, J. J., & Xu, G. X. (2007). A new expression plasmid in Bifidobacterium longum as a delivery system of endostatin for cancer gene therapy. *Cancer gene therapy*, *14(2)*, 151-157.
[19] Corneau, N., Émond, É., & LaPointe, G. (2004). Molecular characterization of three plasmids from Bifidobacterium longum. *Plasmid, 51(2)*, 87-100.
[20] Hu, B., Kou, L., Li, C., Zhu, L. P., Fan, Y. R., Wu, Z. W., ... & Xu, G. X. (2009). Bifidobacterium longum as a delivery system of TRAIL and endostatin cooperates with chemotherapeutic drugs to inhibit hypoxic tumor growth. *Cancer gene therapy*, *16(8)*, 655-663.
[21] Missich, R., Sgorbati, B., & LeBlanc, D. J. (1994). Transformation of Bifidobacterium longum with pRM2, a constructed Escherichia coli-B. longum shuttle vector. *Plasmid*, *32*(2), 208-211.
[22] Nakamura, T., Sasaki, T., Fujimori, M., Yazawa, K., Kano, Y., Amano, J., & Taniguchi, S. I. (2002). Cloned cytosine deaminase gene expression of Bifidobacterium longum and application to enzyme/pro-drug therapy of hypoxic solid tumors. *Bioscience, biotechnology, and biochemistry*, *66*(11), 2362-2366.
[23] Matsumura, H., Takeuchi, A., & Kano, Y. (1997). Construction of Escherichia coli–Bifidobacterium longum shuttle vector transforming B. longum 105-A and 108-A. *Bioscience, biotechnology, and biochemistry*, *61*(7), 1211-1212.
[24] Shkoporov, A. N., Efimov, B. A., Khokhlova, E. V., Steele, J. L., Kafarskaia, L. I., & Smeianov, V. V. (2008). Characterization of plasmids from human infant Bifidobacterium strains: sequence analysis and construction of E. coli–Bifidobacterium shuttle vectors. *Plasmid*, *60*(2), 136-148.
[25] Hou, X., & Liu, J. E. (2006). Construction of Escherichia coli-Bifidobacterium longum shuttle vector and expression of tumor suppressor gene PTEN in B. longum. *Acta microbiologica Sinica*, *46*(3), 347-352.

Part2：Function of apoptin

To verify the inhibitory effect of apoptin on tumor cells, we tested the ability of apoptin to induce apoptosis in tumor cells.

First, we transformed the recombinant plasmid, pGH-apoptin, into E. *coli* BL21 competent bacterium, (Fig.2.1) and detected the expression of apoptin in E. *coli* BL21 by SDS-PAGE (Fig.2.2) and Western Blot (Fig.2.3), which demonstrated that apoptin was expressed successfully in E. *coli* BL21.

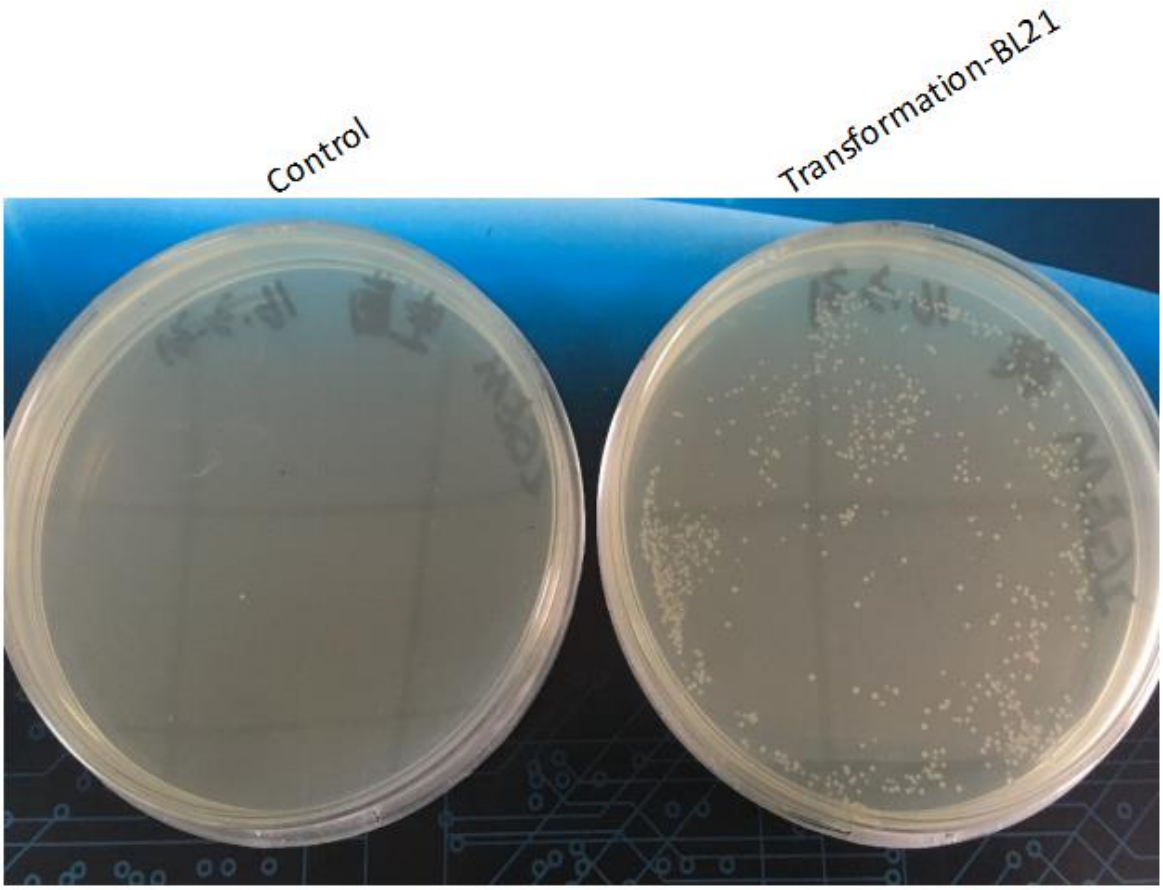

Fig.2.1.The recombinant plasmid pGH–apoptin was transformed into E. *coli* BL21 competent bacterium (selected by Amp^r).

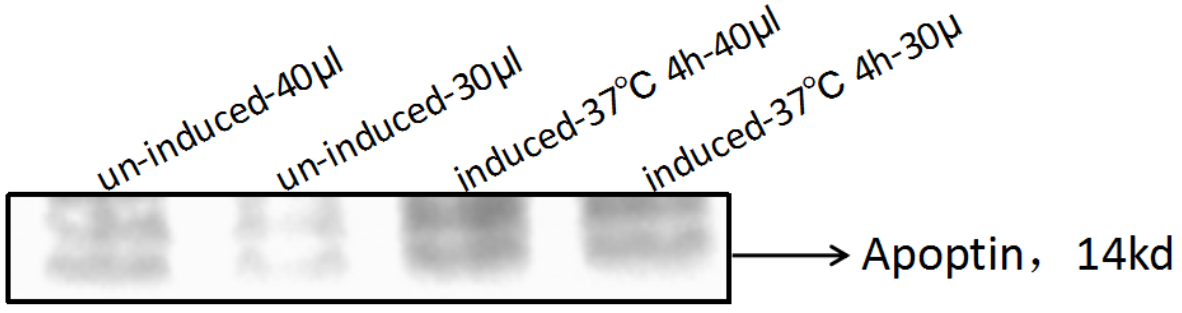

Fig.2.2.The expression of apoptin (13.6kd) was detected through SDS-PAGE. The expression of apoptin in

E. *coli* BL21 was increased in Bl21 cells after induced with IPTG (500mmol/L) in 37℃ for 4h.

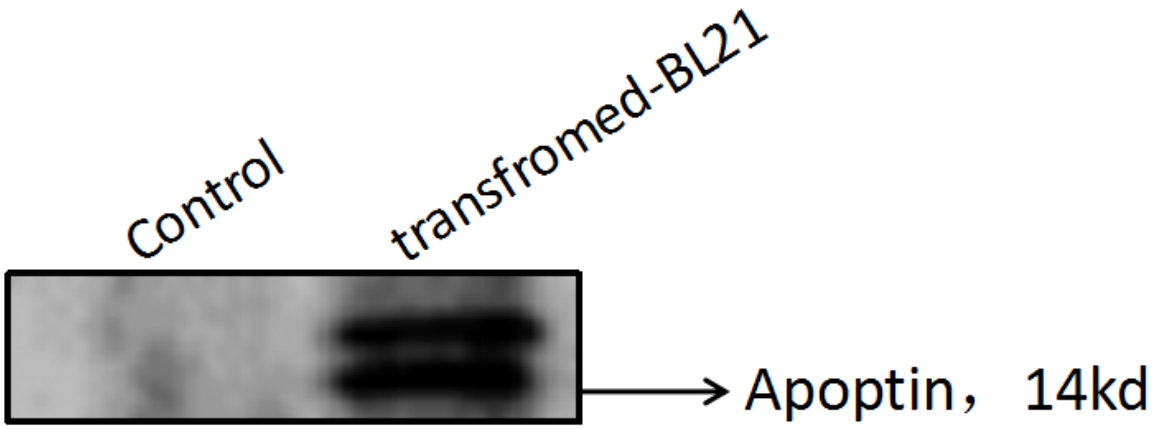

Fig.2.3.The Western Blot analysis demonstrated that the expression of apoptin could only be detected in the transformed BL21 cells.

We transfected pGH-apoptin into MCF-7 (human breast cancer cell) and detected the expression of apoptin in MCF-7 cells by Western Blot (Fig.2.4). We used MTT assay to examine cell proliferation and calculate cell survival rate of MCF-10A (normal human breast epithelial cell) and MCF-7 cells transformed with pGH-apoptin. Apoptin inhibited cell proliferation of MCF-7 cells, but did not affect the growth of MCF-10A cells (Fig.2.5). Wounding-healing assay was used to examine the effects of apoptin on cell migration, which showed that the cell migration ability of MCF-7 cells was affected (Fig.2.6). All these results demonstrated that apoptin is a potential drug for cancer treatment.

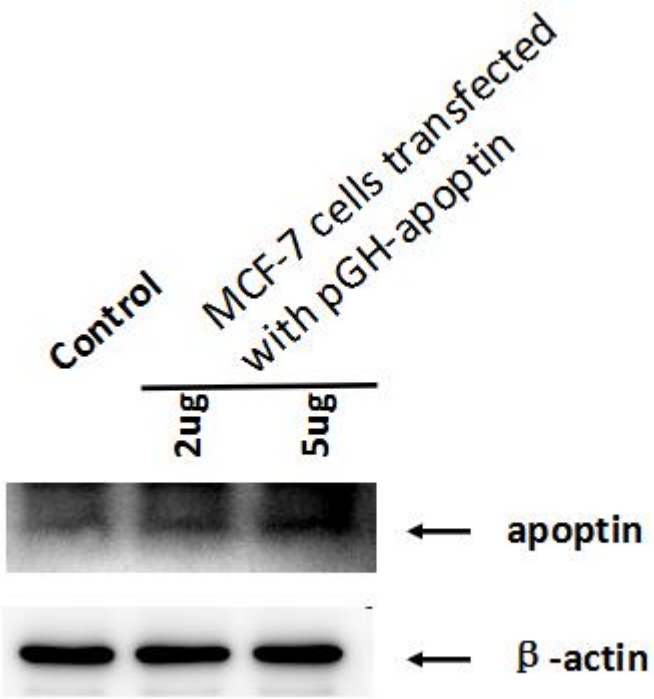

Fig.2.4.The Western Blot indicated that MCF-7 cells can express apoptin after transfection, and the expression was more distinct after MCF-7 cells were transfected with 5 μl plasmid (5 μl) than with 2 μl

plasmid (2 μ l). The expression of apoptin could not be detected in MCF-7 cells without transfection (control).

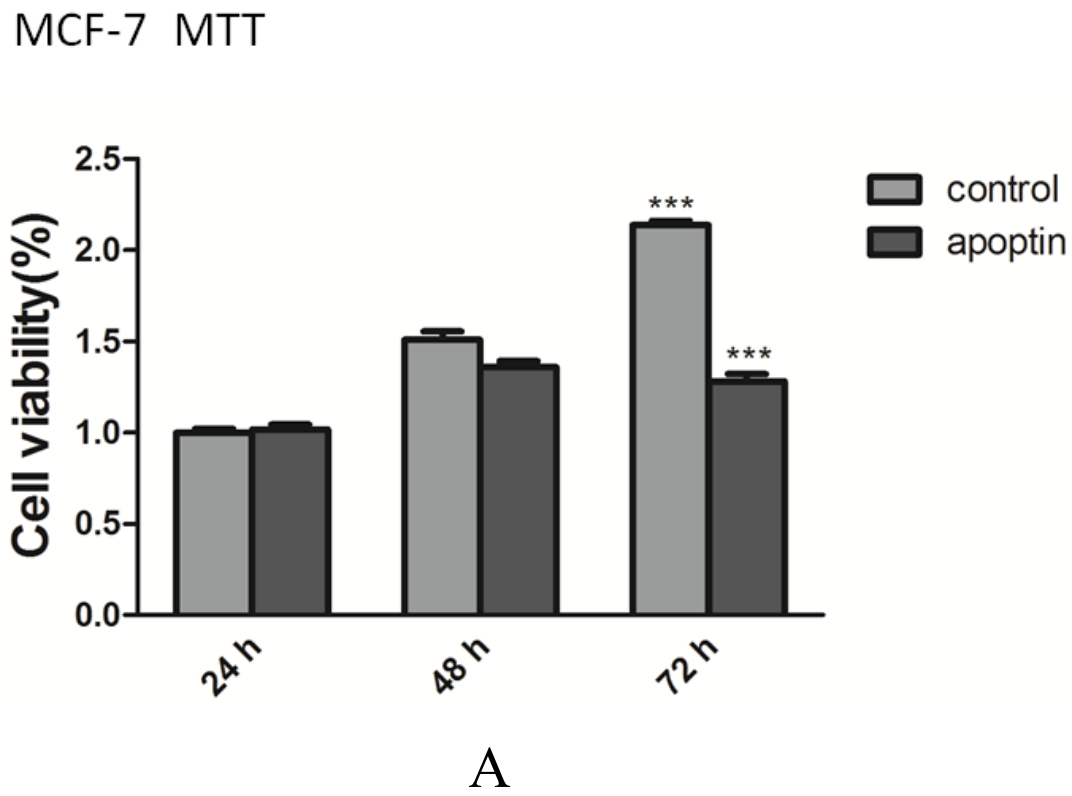

A

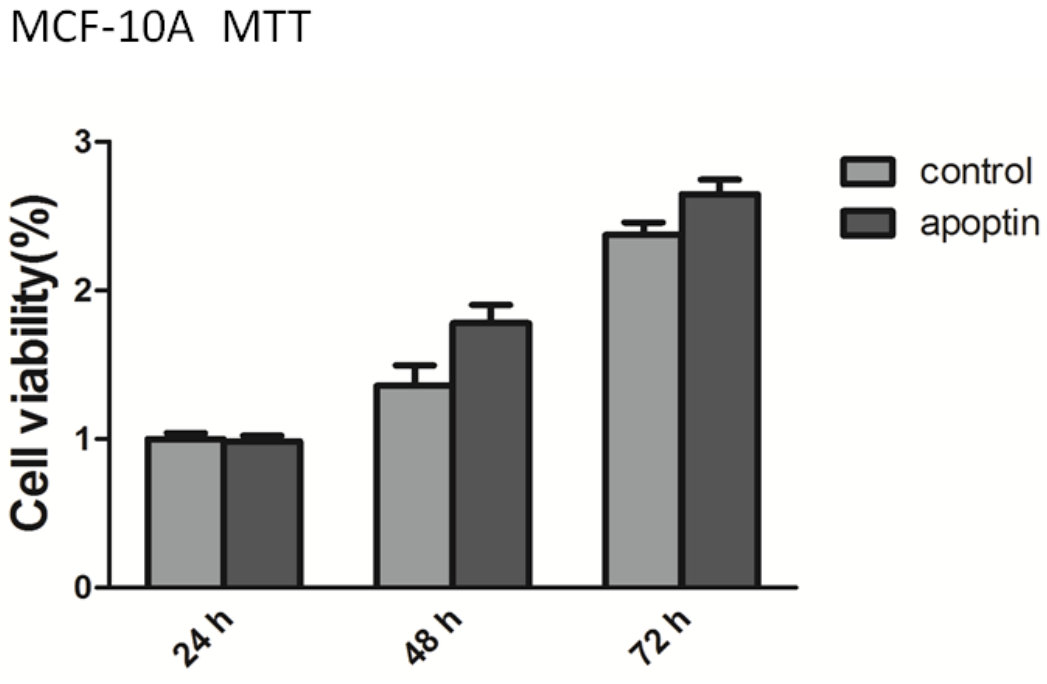

B

Fig.2.5.Apoptin inhibits cell proliferation of MCF-7 cells (A) but not MCF-10A cells (B).

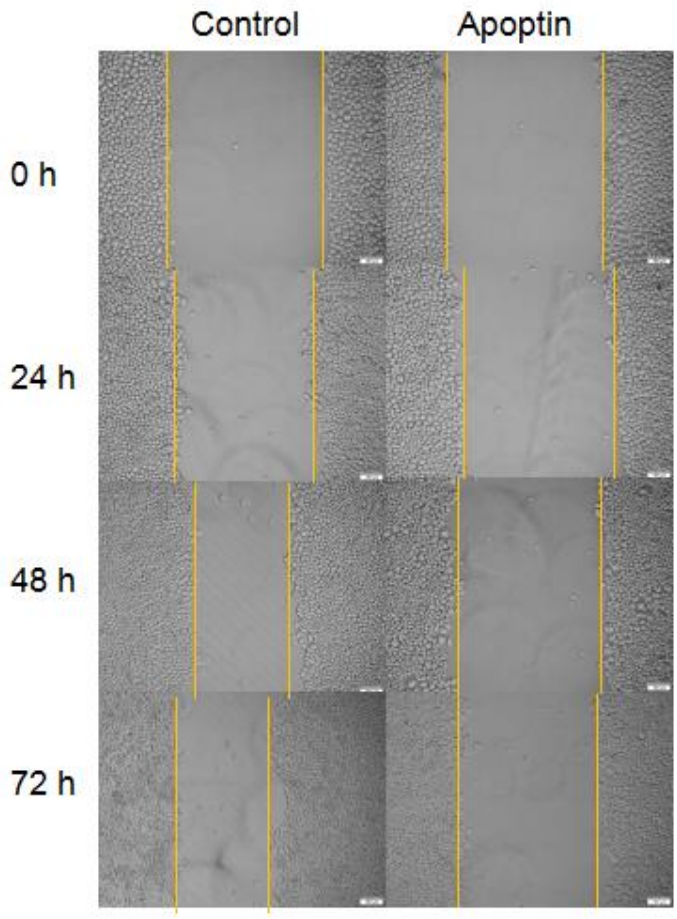

A B

Fig.2.6. The migration ability was decreased in MCF-7 cells transformed with pGH-apoptin.

Part3：Animal experiments

To simulate how our system works in real world condition, we transformed our devices into B. *lougum* and use these engineered Bifidobacterium to treat tumor bearing mice.

First, we transformed our devices (BBa_K1932005, BBa_K1932006, BBa_K1932007) and pUC-18 vector into E. *coli* BL21 competent cells (Fig.3.1). BBa_K1932005 is a device which contains the sequence of TAT-apoptin. BBa_K1932006 is a device which contains the sequence of Sec2-TAT-apoptin and BBa_K1932007 is a device which contains the sequence of Tmp1-TAT-apoptin.

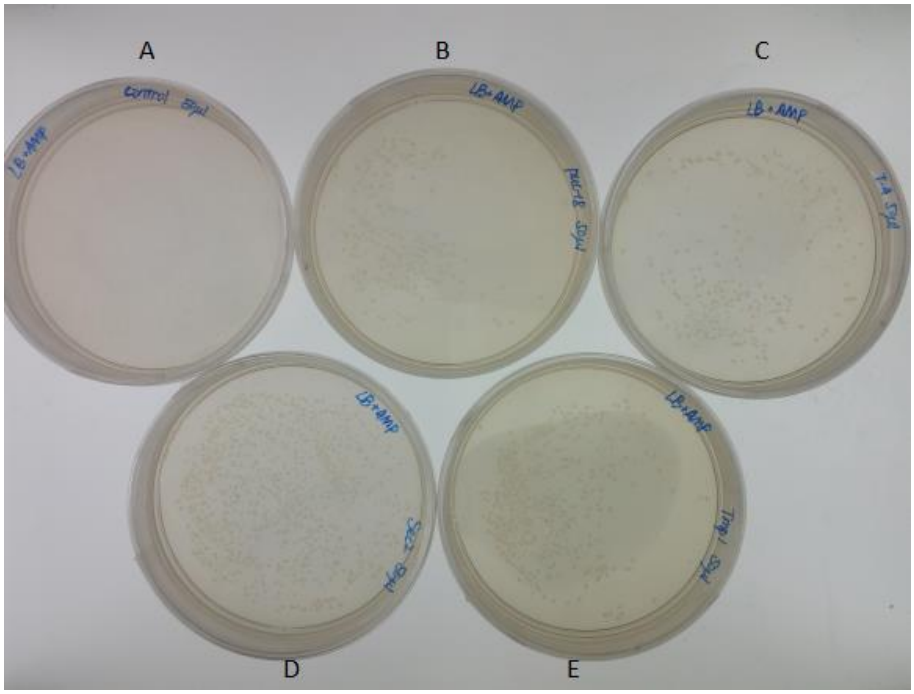

Fig.3.1.Transformation of E. *coli* BL21: control (A), pUC-18 vector (B), pUC-18-TAT-apoptin (C), pUC-18-Sec2-TAT-apoptin (D), pUC-18-Tmp1-TAT-apoptin (E).

Then we transformed two of our devices, BBa_K1932006 and BBa_K1932007, into Bifidobacterium, by electro-transformation assay (Fig.3.2). BBa_K1932006 is a device which contains the sequence of Sec2-TAT-apoptin and BBa_K1932007 is a device which contains the sequence of Tmp1-TAT-apoptin. We used these two devices because each of they contains a signal peptide gene and a TAT trans-membrane domain gene, with which apoptin can be secreted by Bifidobacterium and be transducted into tumor cells. Next, we use a Lyophilizer to lyophilize the solution of these engineered Bifidobacterium in vacuum environment under -50℃. After that we planned to use these lyophilized powder to treat tumor bearing nude mice. So we calculated the CFU (Colony Forming Unit) of our Bifidobacterium lyophilized powder through plate counting (Fig.3.3).

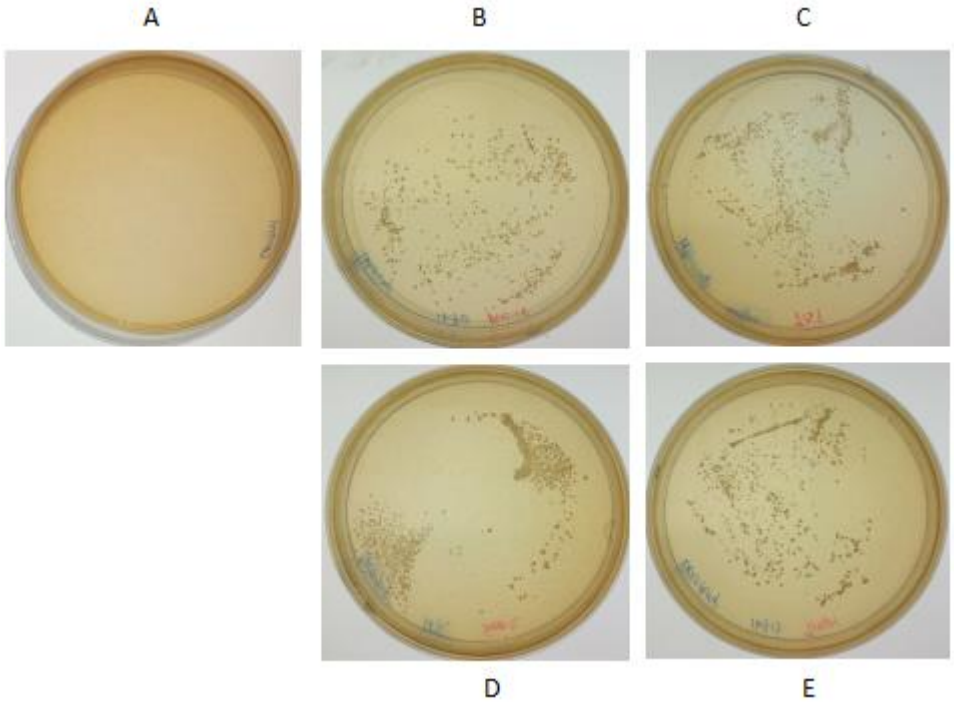

Fig.3.2.Electro-transformation of Bifidobacterium (1250V, 200Ω, 25μf, 1.0mm, 5ms), control (A), pUC-18 vector (B), pUC-18-TAT-apoptin (C), pUC-18-Sec2-TAT-apoptin (D), pUC-18-Tmp1-TAT-apoptin (E).

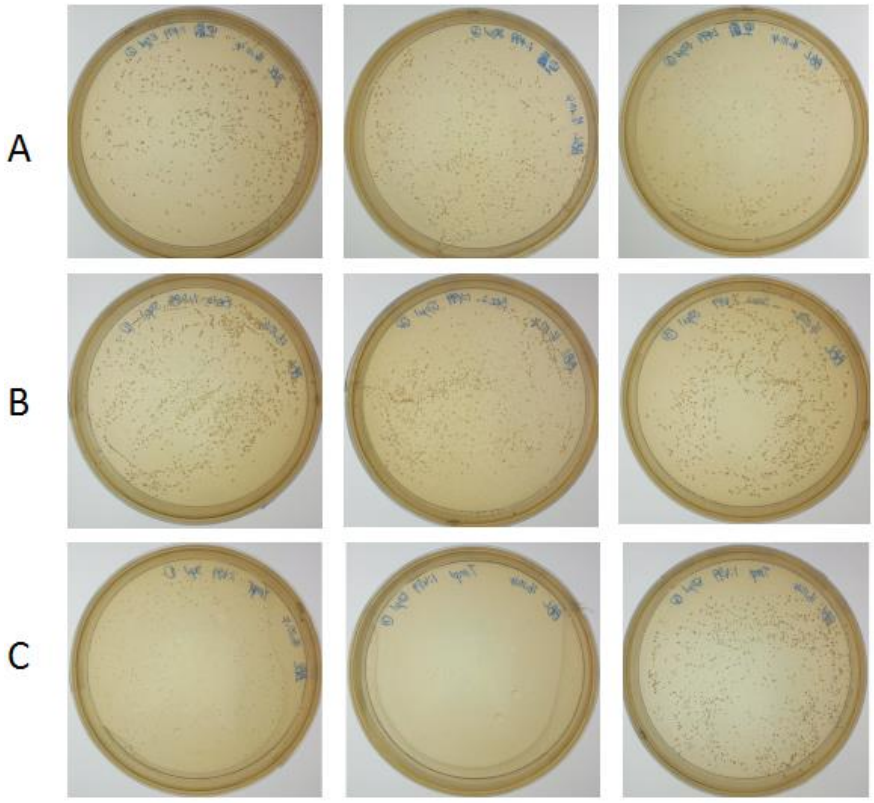

Fig.3.3.The lyophilized powder was diluted with 1 X PBS buffer, and the CFU is calculated by plate counting method, B. *longum* (A), B. *longum* with BBa_K1932006 (pUC-18-Sec2-TAT-apoptin) plasmid (B) B. *longum* with BBa_K1932007 (pUC-18-Tmp1-TAT-apoptin) plasmid (C).

At the same time, we designed the process of constructing a model of liver cancer. Out of the concern of students' safety, undergraduate students are not allowed to enter laboratory animal environment without license. So we outsource these works to JRDUN Biotechnology. They followed our protocol to construct a model of liver cancer using SMMC-7721 cells (human liver cancer cell line). Ten days after they injected 40 nude mice with 100ul SMMC-7721 cell (2×10^7/ml) to axillae, the liver cancer model was constructed. But only 39 tumor bearing nude mice were survived, so we asked them to choose 35 nude mice which have the tumors of similar volume. Then these mice were treated by in situ injection method.

Then these tumor bearing nude mice were divided into five groups randomly (seven for each):

1. NC group, negative control group, injected 50ul 1X PBS buffer in 10d, 15d, and 20d.
2. PC group, positive control group, injected 50ul doxorubicin hydrochloride at a dosage of 4.3769mg/kg in 10d, 15d, and 20d.
3. BF group, Bifidobacterium control group, injected 50ul B. *longum* at a dosage of $2.5\times10^{\wedge}7$ CFU/kg in 10d, 15d, and 20d.
4. BFS group, Bifidobacterium-Sec2 group, injected 50ul injected B. *longum* transformed with BBa_K1932006 at a dosage of $2.5\times10^{\wedge}7$ CFU/kg in 10d, 15d, and 20d.
5. BFT group, Bifidobacterium-Tmp1 group, injected 50ul injected B. *longum* transformed with BBa_K1932007 at a dosage of $2.5\times10^{\wedge}7$ CFU/kg in 10d, 15d, and 20d.

We used the results of plate counting method to dilute the lyophilized powder with 1X PBS buffer, adjusting the concentration of the solution to $1\times10^{\wedge}7$ CFU/ml. To simulate the process of our engineered Bifidobacterium killing tumor cells in vivo, we inject these solutions into tumor-bearing nude mice (Fig.3.4 and Fig.3.5). The volumes of the tumors were measured every three days (Fig.3.6, Tab.1), and tumor mass were weighed at the last day (Fig.3.7, Tab.2).

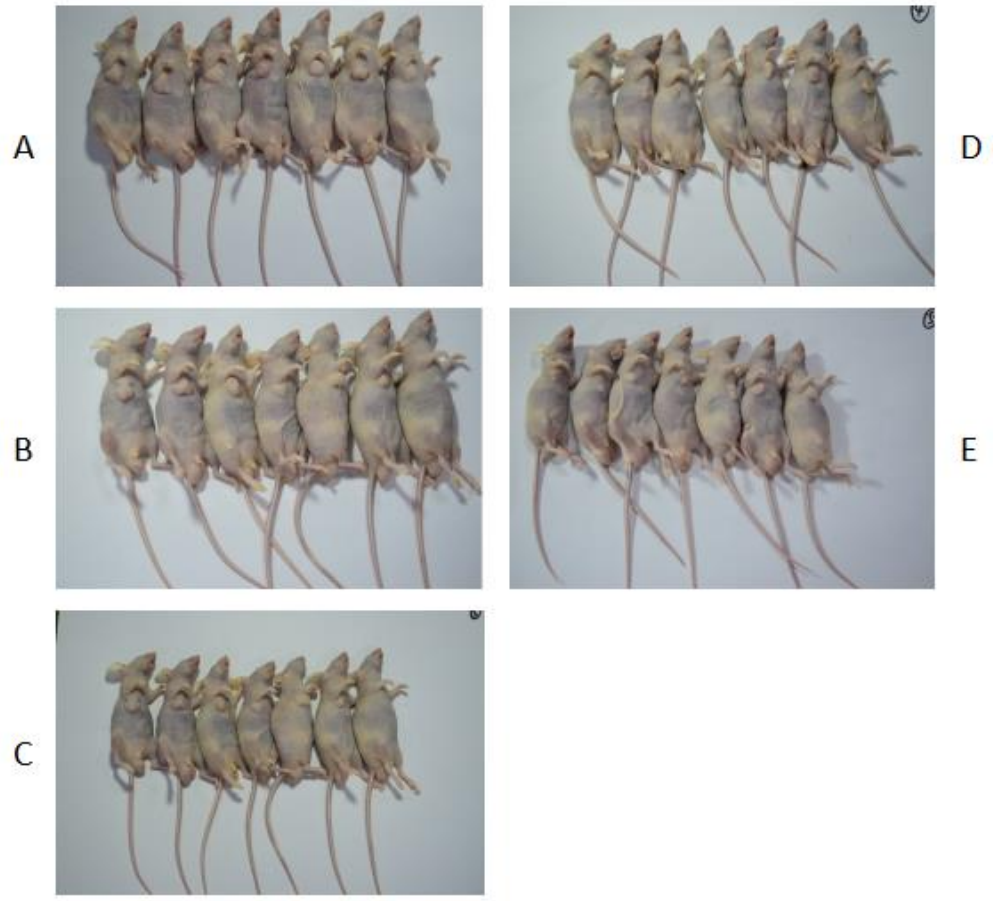

Fig.3.4.Tumor bearing nude mice were injected with the solution of lyophilized powder. (A) Mice in negative control group were injected with 1X PBS buffer. (B) Mice in positive control group were injected with doxorubicin hydrochloride at a dosage of 4.3769mg/kg. (C) Mice in BF group were injected with B. *longum* at a dosage of $2.5\times10^{\wedge}7$ CFU/kg. (D) Mice in BFS group were injected with B. *longum* transformed with BBa_K1932006 at a dosage of $2.5\times10^{\wedge}7$ CFU/kg. (E) Mice in BFT group were injected with B. *longum* transformed with BBa_K1932007 at a dosage of $2.5\times10^{\wedge}7$ CFU/kg.

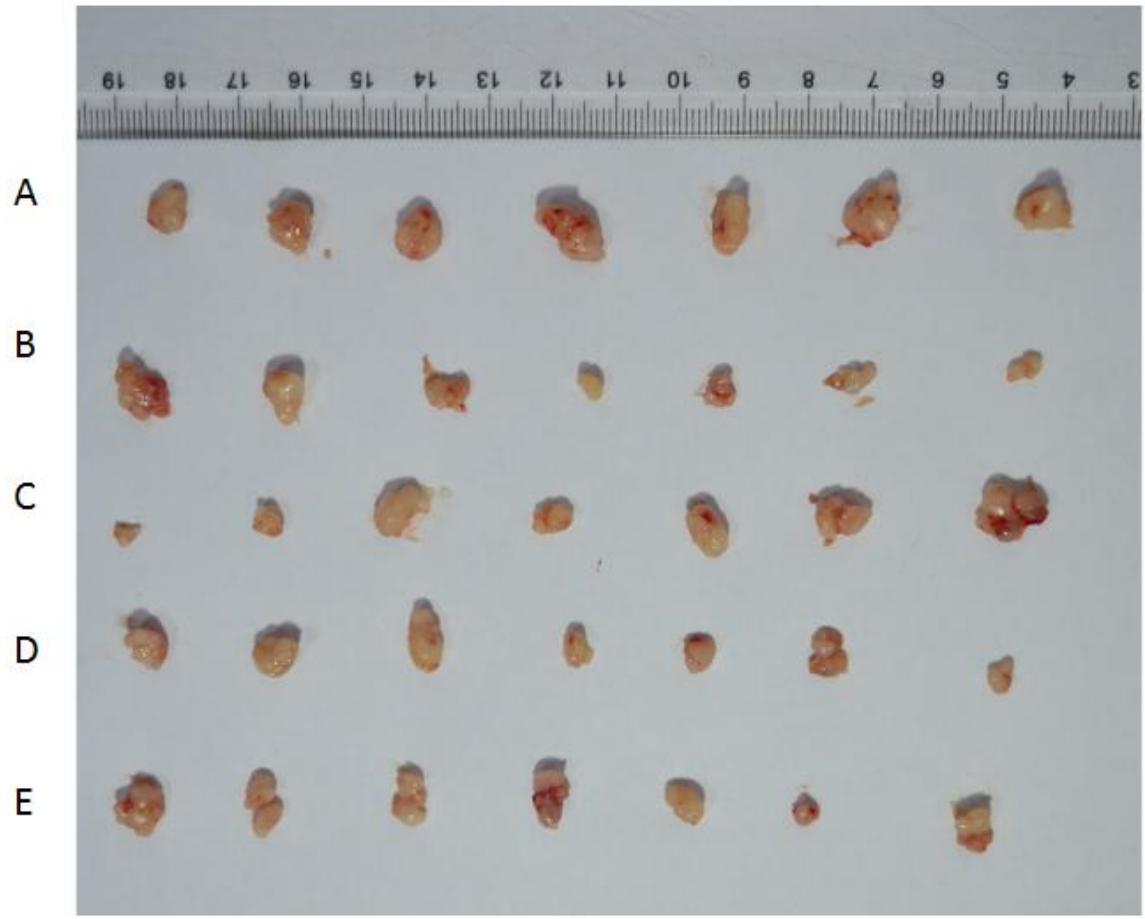

Fig.3.5. Mice were sacrificed by cervical dislocation in 21 days and the tumor mass was photographed. (A) Mice in negative control group were injected with 1X PBS buffer. (B) Mice in positive control group were injected with doxorubicin hydrochloride at a dosage of 4.3769mg/kg. (C) Mice in BF group were injected with B. *longum* at a dosage of $2.5\times10^{\wedge}7$ CFU/kg. (D) Mice in BFS group were injected with B. *longum* transformed with BBa_K1932006 at a dosage of $2.5\times10^{\wedge}7$ CFU/kg. (E) Mice in BFT group were injected with B. *longum* transformed with BBa_K1932007 at a dosage of $2.5\times10^{\wedge}7$ CFU/kg.

A

NC	1		2		3		4		5		6		7	
Days	SD(mm)	LD(mm)	SD(mm)	LD(mm)	SD(mm)	LD(mm)	SD(mm)	LD(mm)	SD(mm)	LD(mm)	SD(mm)	LD(mm)	SD(mm)	LD(mm)
9	1.59	2.38	1.66	1.86	1.74	2.01	1.94	2.47	1.75	1.82	1.53	1.86	1.33	1.42
12	3.67	3.78	3.87	3.96	3.12	3.56	3.02	4.06	3.31	3.45	3.32	3.76	2.5	2.57
15	5.15	5.42	5.65	5.78	5.11	5.86	4.56	6.32	5.23	5.36	4.56	5.44	3.78	3.89
18	6.93	7.51	6.99	7.66	6.72	7.71	6.02	8.87	6.85	6.9	5.5	7.03	4.9	5.15
21	8.58	9.76	9.07	10.57	8.21	10.56	7.42	12.19	8.12	8.36	6.71	9.96	6.53	6.6

B

PC	1		2		3		4		5		6		7	
Days	SD(mm)	LD(mm)	SD(mm)	LD(mm)	SD(mm)	LD(mm)	SD(mm)	LD(mm)	SD(mm)	LD(mm)	SD(mm)	LD(mm)	SD(mm)	LD(mm)
9	1.56	1.83	1.65	1.78	1.84	2.01	1.87	2.1	1.71	2.01	1.69	1.89	1.84	1.91
12	2.71	3.65	2.89	3.02	2.83	3.11	2.91	3.03	3.12	3.28	3.15	3.34	3.18	4.09
15	3.34	4.55	3.95	4.11	3.56	4.23	3.78	3.99	4.07	4.89	4.48	5.51	4.91	5.89
18	4.21	5.12	4.77	5.34	4.37	5.38	4.51	4.86	5.11	6.46	6.08	7.32	6.01	7.53
21	4.91	6.53	5.59	6.44	5.33	6.41	5.61	5.93	6.26	8.23	7.47	9.05	7.08	9.39

C

BF	1		2		3		4		5		6		7	
Days	SD(mm)	LD(mm)	SD(mm)	LD(mm)	SD(mm)	LD(mm)	SD(mm)	LD(mm)	SD(mm)	LD(mm)	SD(mm)	LD(mm)	SD(mm)	LD(mm)
9	1.87	1.92	1.67	2.12	1.77	1.88	1.81	2.02	1.93	1.98	1.57	1.76	1.89	2.05
12	3.98	4.77	3.12	4.56	3.56	4.6	3.28	3.78	3.21	4.67	2.48	2.65	2.48	2.65
15	5.71	6.98	4.53	6.38	6.17	6.3	3.98	5.06	4.47	6.47	3.16	3.54	3.07	3.37
18	7.32	9.01	5.89	8.32	6.3	7.79	4.89	6.21	5.69	8.49	3.79	4.46	3.98	4.09
21	9.74	11.18	7.02	10.43	6.3	9.88	5.87	7.33	6.98	10.55	4.37	5.33	4.83	5.05

D

BFS	1		2		3		4		5		6		7	
Days	SD(mm)	LD(mm)	SD(mm)	LD(mm)	SD(mm)	LD(mm)	SD(mm)	LD(mm)	SD(mm)	LD(mm)	SD(mm)	LD(mm)	SD(mm)	LD(mm)
9	2.01	2.03	1.71	1.85	1.76	1.78	1.74	1.96	1.8	1.97	1.86	1.89	1.78	2.01
12	2.49	3.21	2.38	3.33	3.12	3.31	3.02	3.34	3.46	3.99	3.28	4.05	3.15	3.2
15	3.12	3.99	2.91	4.28	3.96	4.12	3.81	4.13	4.38	5.91	4.39	5.48	4.23	4.32
18	3.74	5.02	3.56	5.19	4.51	4.77	4.84	5.25	5.41	7.83	5.5	6.98	5.39	5.75
21	4.49	6.07	4.27	6.22	5.34	5.46	5.96	6.74	6.46	9.93	6.79	8.65	7.15	7.41

E

BFT	1		2		3		4		5		6		7	
Days	SD(mm)	LD(mm)	SD(mm)	LD(mm)	SD(mm)	LD(mm)	SD(mm)	LD(mm)	SD(mm)	LD(mm)	SD(mm)	LD(mm)	SD(mm)	LD(mm)
9	1.84	1.98	1.69	1.72	1.87	1.98	1.89	2.03	1.74	2.03	1.79	1.91	1.89	2.07
12	3.32	3.45	2.89	3.04	3.18	3.68	3.08	3.74	3.17	4.18	3.67	4.07	4.32	4.34
15	4.51	4.67	3.48	3.56	3.89	4.85	3.55	4.98	3.78	5.48	4.48	5.32	5.47	5.51
18	5.69	5.89	3.96	4.01	4.53	6.19	4.1	6.46	4.65	7.02	5.09	6.9	6.78	6.98
21	6.84	6.98	4.42	4.59	5.36	7.65	4.63	8.07	5.51	9.63	5.76	8.72	8.36	8.41

Tab.1.The volumes of the tumors were measured every three days (Volume=1/2SD*LD^2, SD: short diameter, LD: long diameter). (A) NC group, (B) PC group, (C) BF group, (D) BFS group, (E) BFT group.

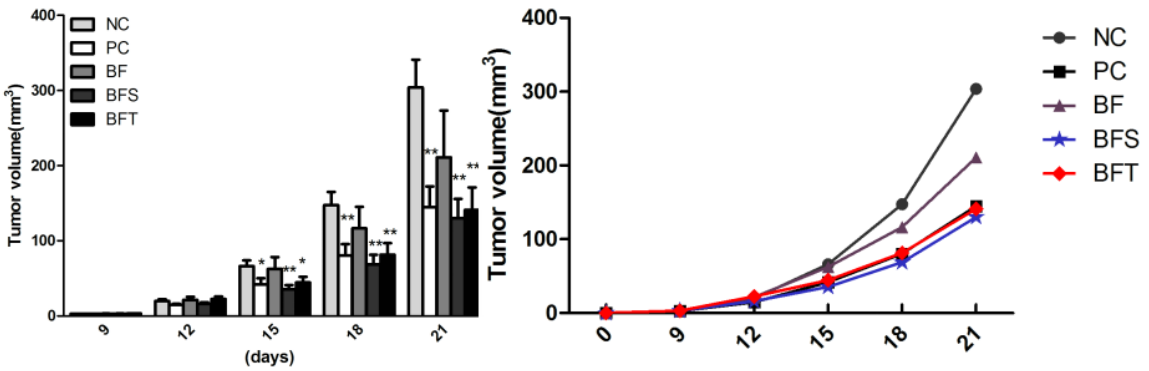

Fig.3.6.The volume of the tumor was measured and recorded every 3 days.

	weight（g）						
Groups	1	2	3	4	5	6	7
NC	0.1387	0.2041	0.1721	0.2801	0.1565	0.1780	0.1077
PC	0.0301	0.0399	0.0327	0.0409	0.0725	0.1619	0.1478
BF	0.2505	0.1546	0.1441	0.0619	0.1697	0.0527	0.0186
BFS	0.0247	0.0546	0.0534	0.0499	0.1483	0.1477	0.1108
BFT	0.1053	0.0212	0.0772	0.1149	0.0886	0.1065	0.1634

Tab.2. The mice were killed by cervical dislocation in 21d and the tumors were weighed.

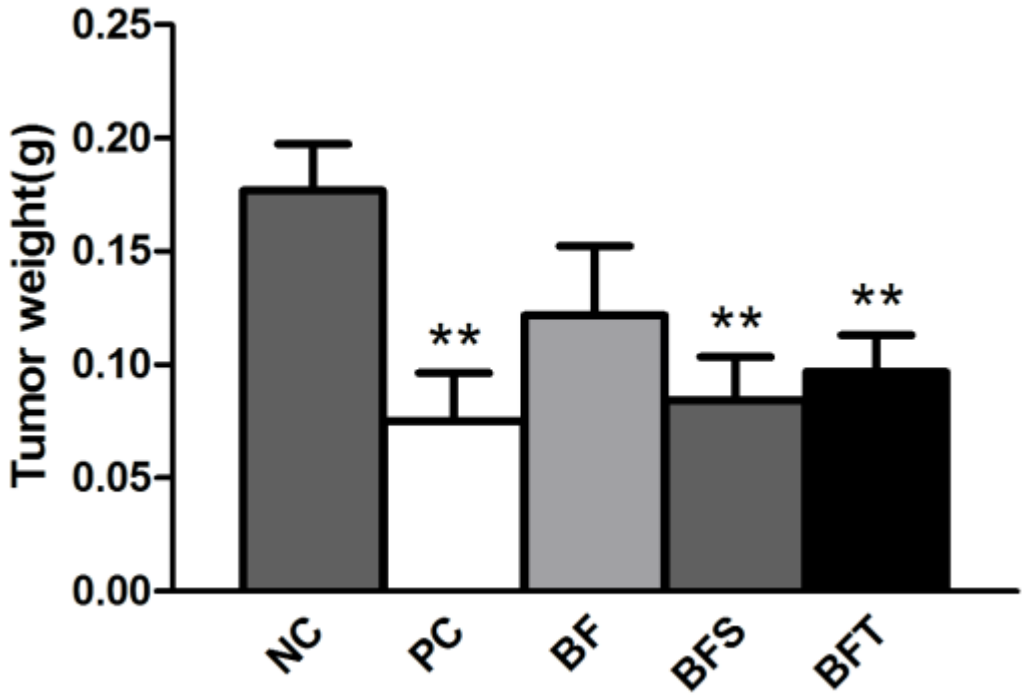

Fig.3.7.The mice were killed by cervical dislocation in 21d and the tumors were weighed.

Compared with NC and BF groups, the tumor growth was retarded in BFS group and BFT group. There was no significant difference on tumor growth between BF group and NC group, indicating *B. longum* alone did not have a significant inhibitory effect on tumor growth.

These results demonstrated that our engineered Bifidobacterium which expresses Sec2-TAT-apoptin protein or Tmp1-TAT-apoptin protein have an inhibiting effect on the growth of solid tumors.